

---

# Revisiting Multivariate Time Series Forecasting with Missing Values

---

Jie Yang<sup>1\*</sup> Yifan Hu<sup>2</sup> Kexin Zhang<sup>3</sup> Luyang Niu<sup>4</sup> Philip S. Yu<sup>1</sup> Kaize Ding<sup>3</sup>

## Abstract

Missing values are common in real-world time series, and multivariate time series forecasting with missing values (MTSF-M) has become a crucial area of research for ensuring reliable predictions. To address the challenge of missing data, current approaches have developed an imputation-then-prediction framework that uses imputation modules to fill in missing values, followed by forecasting on the imputed data. However, this framework overlooks a critical issue: there is no ground truth for the missing values, making the imputation process susceptible to errors that can degrade prediction accuracy. In this paper, we conduct a systematic empirical study and reveal that imputation without direct supervision can corrupt the underlying data distribution and actively degrade prediction accuracy. To address this, we propose a paradigm shift that moves away from imputation and directly predicts based on the partially observed time series. We introduce **Consistency-Regularized Information Bottleneck (CRIB)**, a novel framework built on the Information Bottleneck principle. CRIB combines a unified-variate attention mechanism with a consistency regularization scheme to learn robust representations that filter out noise introduced by missing values while preserving essential predictive signals. Comprehensive experiments on several real-world datasets demonstrate the effectiveness of CRIB, which predicts accurately even under high missing rates. Our code is available in <https://github.com/Muyi1111/CRIB>.

## 1. Introduction

Multivariate time series forecasting (MTSF), which aims to predict future values of multiple variates based on histori-

---

\*Work done during an internship at Northwestern University. <sup>1</sup>University of Illinois Chicago <sup>2</sup>Tsinghua University <sup>3</sup>Northwestern University <sup>4</sup>Tongji University. Correspondence to: Kaize Ding <kaize.ding@northwestern.edu>.

Preprint. February 3, 2026.

cal observations, plays an important role in many domains, such as traffic flow forecasting (Shang et al., 2022; Yu et al., 2017; Bai et al., 2020), financial analysis (Schaffer et al., 2021; Zhu et al., 2024; Li et al., 2025; Hu et al., 2025b;a), and weather prediction (Zheng et al., 2015; Wu et al., 2021; Tan et al., 2022). However, due to uncontrollable factors such as data collection difficulties and transmission failures (Li et al., 2023; Marisca et al., 2022; Cini et al., 2021; Zhang et al., 2025a), real-world multivariate time series data is often partially observed, with missing values scattered throughout the series. These missing values inevitably introduce noise, leading to distribution shifts and disrupting the variate correlations. MTSF models (Cao et al., 2020; Liu et al., 2022; Ekambaram et al., 2023; Hu et al., 2025e), which typically rely on complete data, are highly sensitive to such shifts and correlation destruction, thus failing to make accurate predictions (Zhou et al., 2023; Hu et al., 2025c). This has driven increasing interest in multivariate time series forecasting with missing values (MTSF-M) (Cao et al., 2018; Zuo et al., 2023; Tang et al., 2020), where the objective is to generate accurate and robust forecasts despite the presence of incomplete data.

To mitigate the impact of missing values, recent MTSF-M research (Yu et al., 2025; Peng et al., 2025) has focused on enhancing observed data by imputing missing values to improve prediction performance. One common approach is the two-stage framework, where an imputation module (Wu et al., 2022; Cao et al., 2018; Du et al., 2023) first fills in the missing values, and a forecasting model then predicts future values based on the imputed data (Peng et al., 2025; Chen et al., 2023; Wu et al., 2015). Moreover, to reduce error accumulation between these two stages of two separate models, some studies have proposed an end-to-end framework (Yu et al., 2024; 2025) that imputes missing values progressively during encoding and performs forecasting using the imputed representations. Overall, these methods generally follow an imputation-then-prediction paradigm, aiming to improve forecasting accuracy by mitigating the negative effects of missing values compared to directly applying forecasting models to incomplete data.

However, current MTSF-M methods ignore a critical limitation in real-world applications: **there is no ground truth for missing values**. In such scenarios, the imputation module of the current MTSF-M methods would lack reliable guidance,

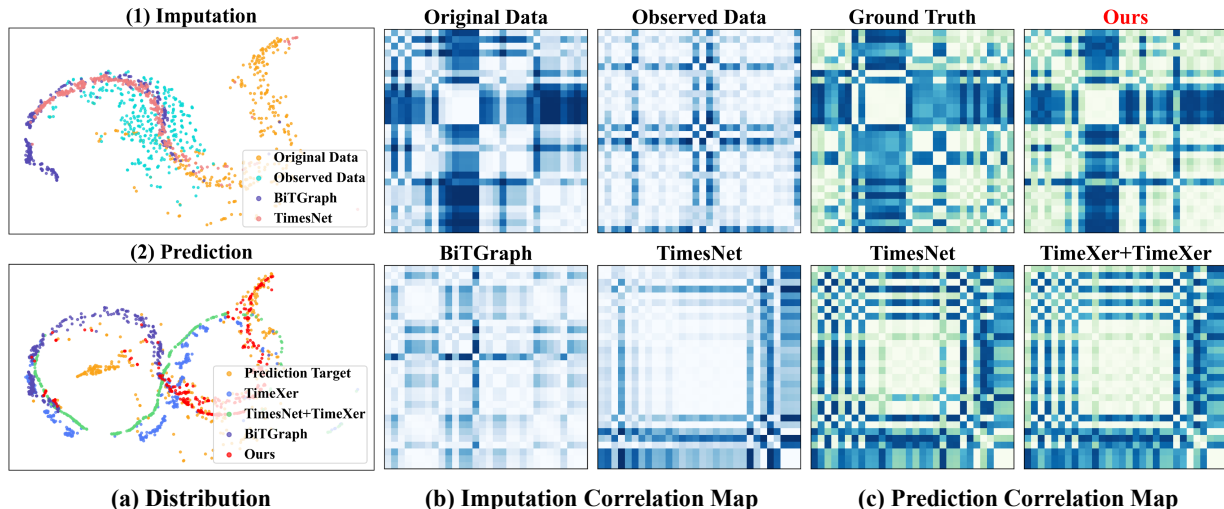


Figure 1. Analysis of the imputation-then-prediction paradigm on PEMS-BAY (40% missing rate). (a) t-SNE visualizations show that current imputation modules cannot recover the original data distribution and their forecasts mismatch with the prediction target, while our direct-prediction method aligns better with the target. (b, c) Correlation maps reveal that imputation fails to recover true variate correlations, whereas our method preserves underlying correlations more effectively. Quantitative analysis is in App. B.

which means the imputed values and reconstructed correlations cannot be guaranteed to be accurate with only the final prediction guidance. As a result, noise would propagate into the prediction stage and degrade forecasting performance, particularly when the missing rate is high. To investigate this issue, we conduct an empirical analysis of representative imputation-then-prediction methods, where original and observed data denote the complete and partially observed data, respectively. This includes the two-stage framework combining TimesNet (Wu et al., 2022) for imputation and TimeXer (Wang et al., 2024a) for forecasting, as well as the end-to-end framework BiTGraph (Chen et al., 2023). Figure 1 illustrates the empirical results, where panel (a) visualizes the distributions of imputed and predicted values, and panels (b) and (c) present the correlations among variates. Our findings highlight two key phenomena:

- ❶ **Improper imputation can corrupt the observed data.** Current MTSF-M frameworks commonly employ imputation modules to recover missing values. However, as shown in Figure 1 (a-1, b), without enough direct supervision, imputed values deviate considerably from the distribution of the original complete data, and the underlying correlations among variates are not correctly reconstructed. The deterioration of both the data distribution and variate correlations suggests that imputation guided only by the prediction objective can degrade the observed data rather than effectively repairing the missing values.
- ❷ **Flawed imputation, in turn, leads to poor prediction performance.** Errors from the imputation stage inevitably propagate into forecasting. As shown in Figure 1 (a-2, c), the predictions exhibit large deviations from the prediction

targets. Notably, even a model TimeXer applied directly to incomplete observed data outperforms a more complex framework that combines TimesNet for imputation with TimeXer for prediction. These findings indicate that a flawed imputation stage can actively harm, rather than enhance, the forecasting capabilities of a model.

Based on these two observations, we ask a fundamental question: *Is it possible to predict directly from partially observed time series, avoiding the pitfalls of imputation while maintaining high accuracy?* To answer this, we propose Consistency-Regularized Information Bottleneck (CRIB), a novel framework that predicts directly from partially observed data, bypassing the issues associated with imputation. CRIB is built on the Information Bottleneck (IB) principle, which enables it to learn a compressed representation that filters noise from missing values while preserving essential predictive signals. To achieve this, it employs a unified-variate attention mechanism to capture complex correlations from the sparse input and is trained with a consistency regularization scheme to enhance robustness, especially under high missing rates.

Our main contributions can be summarized as follows:

- **Empirical analysis:** We perform a systematic empirical study of dominant imputation-then-prediction paradigms for MTSF-M, showing that imputation modules guided only by the prediction objective can corrupt the observed data distribution and degrade prediction performance.
- **Method:** We propose a novel direct-prediction method, CRIB, which removes the imputation step completely.

Built on the Information Bottleneck principle, CRIB integrates unified-variate attention and consistency regularization to learn refined representations that balance noise filtering and task-relevant information preservation.

- **Experiments:** Extensive experiments on four real-world benchmarks demonstrate that CRIB significantly outperforms state-of-the-art methods by an average of 18%, particularly under high missing rates, highlighting the advantage of direct prediction over imputation-then-prediction.

## 2. Preliminaries

**Notations & Problem Formulation** In MTSF-M tasks, the historical time series is denoted as  $X = \{x_i^{1:T} \mid i = 1, \dots, N\} \in \mathbb{R}^{N \times T}$ , where  $T$  is the number of time steps and  $N$  is the number of variates. The goal is to predict the future  $S$  time steps  $Y = \{x_i^{T+1:T+S} \mid i = 1, \dots, N\} \in \mathbb{R}^{N \times S}$ . Missingness is represented by a binary mask  $M \in \{0, 1\}^{N \times T}$ , where  $X^o = \{X^{i,j} \mid M^{i,j} = 1\}$  are observed values and  $X^m = \{X^{i,j} \mid M^{i,j} = 0\}$  are missing values. We denote  $Z \in \mathbb{R}^{N \times D}$  as the intermediate representations of input, where  $D$  is the dimension of the representation.

**Information Bottleneck for MTSF-M** IB theory (Tishby & Zaslavsky, 2015; Voloshynovskiy et al., 2019; Yang et al., 2025) provides an information-theoretic framework for learning compact yet informative representations. Given the partially observed input  $X^o$  and prediction target  $Y$ , the goal is to learn a latent representation  $Z$  that compresses  $X^o$  while preserving maximal information about  $Y$ . This trade-off in CRIB is formalized as follows:

$$\min_{\theta} [I_{\theta}(Z; X^o) - \beta \cdot I_{\theta}(Y; Z)]. \quad (1)$$

Here,  $\theta$  represents the learnable parameters of our proposed CRIB.  $I(Z; X^o)$  and  $I(Y; Z)$  are the mutual information terms measuring compactness and informativeness, respectively. The Lagrange multiplier  $\beta \in \mathbb{R}^+$  controls the balance between these two terms (Tishby et al., 2000). Furthermore, under standard assumptions in the IB literature (Alemi et al., 2016; Chalk et al., 2016; Ma et al., 2023), the joint distribution of the variables can be factorized as:

$$\begin{aligned} p(X^o, Y, Z) &= p(Z \mid X^o, Y) p(Y \mid X^o) p(X^o) \\ &= p(Z \mid X^o) p(Y \mid X^o) p(X^o), \end{aligned} \quad (2)$$

namely, there is a Markov chain  $Y \leftrightarrow X^o \leftrightarrow Z$ , indicating that the representations  $Z$  is learned only from  $X^o$  without direct access to the target  $Y$ .

## 3. Methodology

As illustrated in Figure 2, our proposed model, CRIB, bypasses the problematic imputation stage by performing fore-

casts directly on the partially observed data. The architecture is composed of several key stages, each designed to address the challenges of learning from partially observed data. First, to handle the raw, sparse input, we introduce a Patching Embedding layer that employs a Temporal Convolutional Network (TCN) (Bai et al., 2018) to learn robust local feature representations from available data points. Second, to capture the complex global correlations that are disrupted by missingness, a Unified-Variate Attention mechanism models correlations across all patches simultaneously. Third, to ensure the model learns features that are stable and invariant to different missingness, especially under high missing rates, we introduce a Consistency Regularization scheme based on data augmentation. The entire learning process is guided by the IB principle, which provides a theoretical foundation for learning a representation that is maximally compressive against noise while being sufficiently informative for the forecasting task.

### 3.1. Patching Embedding

To effectively enhance the semantic information that is not available in the partially observed, point-level time series  $X^o \in \mathbb{R}^{N \times T}$ , we first transform the input into a sequence of more meaningful patch-level representations (Nie et al., 2022). The series is partitioned into non-overlapping patches  $\hat{X} = \{\hat{x}_i^{1:T/P} \mid i = 1, \dots, N\} \in \mathbb{R}^{N \times (T/P) \times P}$  of length  $P$ . We choose  $P$  such that the total length  $T$  is evenly divisible. Consequently, this patching strategy reduces the sequence length from  $T$  to  $T/P$ , thus remarkably lowering the memory and computational cost of attention calculation.

Next, to enable the following unified-variate attention mechanism to capture the temporal directionality of each variate  $x_i^{1:T}$ , we adopt the temporal encoding strategy inspired by vanilla transformer (Vaswani, 2017) as follows:

$$\text{TE}(t, m) = \begin{cases} \sin(t/10000^{2m/P}) & \text{if } m = 2k, \\ \cos(t/10000^{2m/P}) & \text{if } m = 2k + 1, \end{cases} \quad (3)$$

where  $m$  represents the  $m$ -th dimension of the feature. These temporal embeddings are added to the input patches to provide temporal information. Each patch, now containing a mix of observed values and temporal embeddings, is then processed by a TCN. It utilizes its efficient dilated convolution structure to transform sparse patches with missing values into dense feature representations  $H \in \mathbb{R}^{N \times (T/P) \times D}$  that capture local temporal correlations.

### 3.2. Unified-Variate Attention

To model the complex, non-local correlations disrupted by missing data, we introduce a unified attention mechanism. Instead of using separate modules for inter- and intra-variate correlations among all the variates, our approach treats all patch representations uniformly. We first flatten the patch

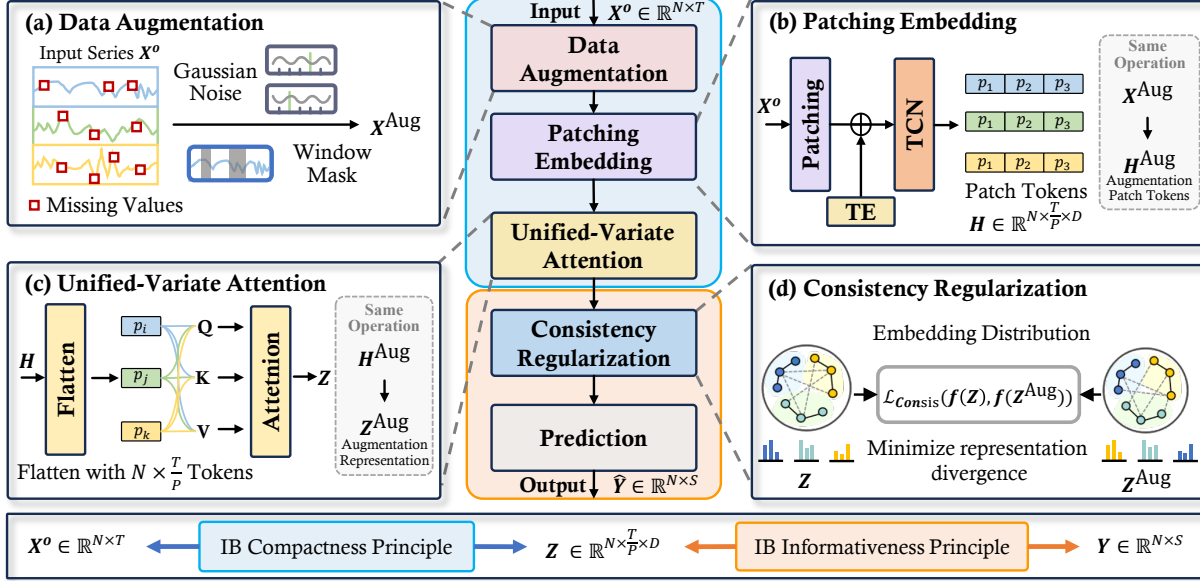


Figure 2. Overall framework of CRIB. (a) Data Augmentation creates a more challenging view of the partially observed data  $X^o$  by generating an augmented version  $X^{Aug}$ . (b) The Patching Embedding layer converts the  $X^o$  and  $X^{Aug}$  into robust patch-level feature representations  $H$  and  $H^{Aug}$ . (c) The Unified-Variate Attention mechanism models the global correlations between all the patches within  $H$  and  $H^{Aug}$  to produce refined representations  $Z$  and  $Z^{Aug}$ . (d) Consistency Regularization aligns the representations from the original  $Z$  and the augmented views  $Z^{Aug}$ . The entire process is guided by the IB principles of compactness and informativeness to predict  $\hat{Y}$ .

representations  $H$  into a sequence  $\hat{H} \in \mathbb{R}^{(N \times T/P) \times D}$  with  $N \times T/P$  tokens. A standard self-attention mechanism is then applied to this flattened sequence:

$$Z = \text{Attention}(Q, K, V) = \text{Softmax}\left(\frac{QK^\top}{\sqrt{D}}\right)V, \quad (4)$$

where  $Q, K, V \in \mathbb{R}^{(N \times T/P) \times D}$  are the linear projections of tokens  $\hat{H}$ , and  $\top$  denotes the matrix transpose. This allows the model to learn all possible correlations—both within a single variate’s timeline (intra-variate) and across different variates (inter-variate)—without imposing strong, predefined structural biases. Such flexibility is particularly advantageous for sparse data, as it permits the model to rely on the most informative available signals, regardless of their origin. Unlike previous methods (Yi et al., 2024; Wang et al., 2024b) that employ strategies to reduce the memory and time costs of attention calculations, often at the expense of attention mechanism performance, we accelerate attention computation by patching time series. This can reduce the number of temporal tokens from  $T$  to  $T/P$ , lowering the memory and computational cost of attention calculation by a factor of  $P^2$ , while enhancing the semantic-level information of the data.

### 3.3. Final Prediction

In CRIB, we implement the predictor using a simple Multi-Layer Perceptron (MLP) as follows:

$$\hat{Y} = \text{Predictor}(Z) = \text{MLP}(Z) \in \mathbb{R}^{N \times S}, \quad (5)$$

where  $S$  is the prediction length and  $\text{MLP}(\cdot)$  denotes a simple two-layer fully connected network with a ReLU activation function applied between the layers. We deliberately employ a simple linear predictor to demonstrate that the forecasting performance of CRIB stems from the high-quality, robust representations  $Z$  learned by our IB-guided attention mechanism, rather than employing a complex and powerful predictor (Liu et al., 2023; Zeng et al., 2023).

### 3.4. Information Bottleneck Guidance

To enhance the quality of the learned representations  $Z$  and improve forecasting accuracy, we propose an IB-based guidance. This guidance aims to balance compactness (filtering out irrelevant information) with informativeness (preserving relevant task-specific signals), allowing CRIB to focus on the most significant factors for accurate forecasting. In this section, we present how the compactness and informativeness principles are formulated and implemented in our framework. Full derivations are detailed in App. A.

#### 3.4.1. COMPACTNESS PRINCIPLE

The compactness principle, which aims to minimize the mutual information  $I_\theta(Z; X^o)$ , forces the learned representation  $Z$  to be a minimal sufficient statistic of the input. In our context, this encourages the model to discard non-essential information, which critically includes the noise introduced by the arbitrary locations of missing values. Following the variational inference (Voloshynovskiy et al., 2019), we

derive a equivalent form of the compactness term in Eq. 1:

$$\begin{aligned} I_\theta(Z; X^\circ) &= \mathbb{E}_{p(x^\circ, z)} \left[ \log \frac{p(x^\circ, z)}{p(z)p(x^\circ)} \right] \\ &= \mathbb{E}_{p(x^\circ)} [D_{\text{KL}}(p(z | x^\circ) \| q(z))] \\ &\quad - D_{\text{KL}}(p(z) \| q(z)). \end{aligned} \quad (6)$$

Because of difficulty in posterior calculation and the non-negative property of Kullback-Leibler (KL) divergence, we use  $p_\theta(z|x^\circ)$  to approximate the true posterior distribution  $p(z|x^\circ)$  and bound Eq. 6:

$$I_\theta(Z; X^\circ) \leq \mathbb{E}_{p(x^\circ)} D_{\text{KL}}[p_\theta(z|x^\circ) \| q(z)] \stackrel{\text{def}}{=} \mathcal{L}_{\text{Comp}}, \quad (7)$$

where we set isotropic Gaussian as the prior distribution of refined representations  $Z$ , i.e.,  $p(Z) = \mathcal{N}(0, I)$ . Therefore, representations  $Z$  are produced through a multivariate Gaussian distribution as:

$$p_\theta(Z|X^\circ) = \mathcal{N}(\mu_\theta(X^\circ), \text{diag}(\delta_\theta(X^\circ))), \quad (8)$$

where  $\mu_\theta(\cdot)$  and  $\sigma_\theta(\cdot)$  are designed as neural networks with parameter  $\theta$ . For training, we use the standard reparameterization trick (Kingma, 2013),  $Z = \mu_\theta(X^\circ) + \sigma_\theta(X^\circ) \odot \epsilon$ , which makes the objective in Eq. 7 differentiable without the need for stochastic estimation as follows:

$$\begin{aligned} \mathcal{L}_{\text{Comp}} &= \frac{1}{2} \sum_{j=1}^D \left( 1 + \log(\sigma_\theta^{(j)}(X^\circ))^2 \right. \\ &\quad \left. - (\mu_\theta^{(j)}(X^\circ))^2 - (\sigma_\theta^{(j)}(X^\circ))^2 \right). \end{aligned} \quad (9)$$

Here,  $\mu_\theta^{(j)}(X^\circ)$  and  $\sigma_\theta^{(j)}(X^\circ)$  denote the  $j$ -th element of the mean and standard deviation vectors.

### 3.4.2. INFORMATIVENESS PRINCIPLE

To balance the compactness objective, the informativeness principle ensures that the representation  $Z$  preserves sufficient information for the forecasting task. To derive a tractable lower bound for the informativeness term, we follow the framework in (Voloshynovskiy et al., 1912) and Eq. 2, and assume that prediction errors follow a Gaussian distribution with fixed variance  $\sigma^2$ , i.e.,  $q_\theta(y|z) = \mathcal{N}(\hat{y}, \sigma^2 I)$  (Choi & Lee, 2023). The derivation proceeds as:

$$\begin{aligned} I_\theta(Y; Z) &= \mathbb{E}_{p(z, y)} \left[ \log \frac{q_\theta(y|z)}{p(y)} \right] + \mathbb{E}_{p(z, y)} \left[ \log \frac{p(y|z)}{q_\theta(y|z)} \right] \\ &\geq \mathbb{E}_{p(z, y)} [\log q_\theta(y|z)] \\ &= -\mathbb{E}_{p(z, y)} \left[ \frac{1}{2\sigma^2} \|y - \hat{y}\|^2 + \frac{T}{2} \log(2\pi\sigma^2) \right] \\ &\propto -\mathbb{E}_{p(z, y)} [\|y - \hat{y}\|^2] \stackrel{\text{def}}{=} -\mathcal{L}_{\text{Pred}}. \end{aligned} \quad (10)$$

thus encouraging the model to extract task-relevant information from intermediate representations.

### 3.5. Consistency Regularization

While the IB framework encourages learning a compact representation, high missing rates can still lead to unstable training as shown in App. E.2, where the model overfits to the specific variate in a given time window (Choi & Lee, 2023). To mitigate this and enhance robustness, we introduce a consistency regularization scheme (Bachman et al., 2014; Laine & Aila, 2016). The core intuition is that the model’s prediction should be invariant to the missingness. We achieve this by creating an augmented, more challenging view of the input, e.g. introducing additional noise to partially observed data. By enforcing that the representations learned from the observed and augmented views remain consistent, we regularize the model to handle missing values while stabilizing the refined representations instead of focusing excessively on a limited subset of observed data and neglecting crucial task-relevant variate correlations.

**Data Augmentation** Specifically, we generate  $X^{\text{Aug}} \in \mathbb{R}^{N \times T}$  by applying two augmentations (Wen et al., 2020): (1) Random Masking, where we randomly select an additional 10% of the observed time points and set them to zero to simulate a more severe missingness scenario; and (2) Gaussian Noise, where we add noise  $\epsilon \in \mathcal{N}(0, I)$  to all observed points to simulate sensor noise, enhancing the model’s robustness to minor fluctuations in the input..

**Consistency Regularization** Then, through the same forward process as  $X^\circ$ , we can get their refined representations  $Z^{\text{Aug}}$ . The refined representations of observed and augmented data are regularized via the following consistency regularization loss function:

$$\mathcal{L}_{\text{Consis}} = \frac{1}{N \times T/P} \sum_{i=1}^{N \times T/P} \|z_i - z_i^{\text{Aug}}\|^2, \quad (11)$$

where  $N \times T/P$  is the number of the flattened tokens. By aligning the representations of the observed and augmented data, the model is encouraged to learn stable representations, thus enhancing robustness in scenarios with high missing rates. Furthermore, this consistency regularization can be seamlessly integrated into the overall optimization objective, complementing the IB theory to ensure that the refined representations retain essential task-relevant information while filtering out irrelevant noise from the missing values.

### 3.6. Model Learning

We have proposed a consistency-regularized method CRIB, which can complete MTSF-M tasks based on the IB theory. Overall, we optimize our model based on the following objective by combining all the introduced loss functions:

$$\min_{\theta} [\alpha \cdot (\mathcal{L}_{\text{Comp}}^\theta + \beta \cdot \mathcal{L}_{\text{Pred}}^\theta) + \gamma \cdot \mathcal{L}_{\text{Consis}}], \quad (12)$$

Table 1. Performance comparison on four datasets with a point missing pattern (average MAE and MSE across 20% to 70% missing rate). Best is **Bold** and second-best is Underlined.

Data	Metric	BiTGraph	BRITS	GRIN	SAITS	SPIN	SegRNN		WPMixer		iTransformer		PatchTST		DLinear		TimeXer		PAtn	Ours	IMP	
		Original	Original	Original	Original	Original	Original	Imputed	Original	Imputed	Original	Imputed	Original	Imputed	Original	Imputed	Original	Imputed	Original	Original		
PEMS-BAY	MAE	0.413	0.366	0.350	OOM	0.402	0.120	0.178	0.155	0.201	<u>0.107</u>	0.125	0.129	0.139	0.156	0.148	0.125	0.135	0.110	0.148	<b>0.093</b>	<b>13%</b>
	MSE	0.788	0.705	0.623	OOM	0.649	0.067	0.203	0.082	0.140	0.055	0.072	0.060	0.086	0.087	0.081	<u>0.051</u>	0.073	0.061	0.091	<b>0.043</b>	<b>15%</b>
Metr-LA	MAE	0.445	0.366	0.389	0.451	0.625	0.318	0.314	0.356	0.342	<u>0.273</u>	0.290	0.313	0.306	0.399	0.366	0.321	0.298	0.302	0.294	<b>0.262</b>	<b>4%</b>
	MSE	0.760	0.611	0.653	0.721	0.965	0.345	0.360	0.356	0.385	0.317	0.330	0.320	0.349	0.373	0.362	<u>0.313</u>	0.333	0.337	0.345	<b>0.301</b>	<b>4%</b>
ETTh1	MAE	0.337	0.357	0.356	0.372	0.437	0.356	0.425	0.340	0.399	0.342	0.419	0.324	0.386	0.402	0.598	<u>0.314</u>	0.347	0.341	0.432	<b>0.256</b>	<b>18%</b>
	MSE	0.387	0.421	0.400	0.457	0.468	0.479	0.477	0.432	0.417	0.408	0.473	0.385	0.435	0.560	0.682	0.377	<u>0.370</u>	0.416	0.470	<b>0.269</b>	<b>27%</b>
Electricity	MAE	0.036	0.035	0.034	0.053	0.136	0.078	0.255	0.049	0.218	0.034	0.130	0.036	0.105	0.074	0.210	<u>0.029</u>	0.083	0.042	0.152	<b>0.026</b>	<b>10%</b>
	MSE	0.113	0.059	0.061	0.266	0.358	1.010	1.286	0.172	0.286	<u>0.054</u>	0.547	0.092	0.379	0.404	2.000	0.064	0.100	0.115	0.864	<b>0.044</b>	<b>18%</b>

Table 2. Performance comparison on six additional datasets with a point missing pattern (average MAE and MSE across 20% to 70% missing rate). Best is **Bold** and second-best is Underlined.

Data	Metric	SegRNN	WPMixer	iTransformer	PatchTST	DLinear	PAtn	CSDI	NeuralCDE	ImputeFormer	TimesNet	Ours
ETTh2	MAE	0.163	0.171	0.225	0.182	0.225	0.211	0.519	0.320	<u>0.152</u>	0.182	<b>0.141</b>
	MSE	0.061	0.066	0.124	0.090	0.117	0.106	0.684	0.188	<u>0.054</u>	0.076	<b>0.048</b>
ETTm1	MAE	<u>0.339</u>	0.381	0.398	0.377	0.505	0.389	0.658	0.498	0.400	0.361	<b>0.313</b>
	MSE	<u>0.526</u>	0.637	0.671	0.606	0.967	0.638	1.284	0.853	0.601	0.565	<b>0.453</b>
ETTm2	MAE	0.130	0.153	0.206	0.182	0.217	0.190	0.527	0.234	<u>0.123</u>	0.170	<b>0.116</b>
	MSE	0.041	0.054	0.113	0.092	0.107	0.098	0.681	0.110	<u>0.037</u>	0.065	<b>0.034</b>
Weather	MAE	<u>0.059</u>	0.087	0.118	0.121	0.171	0.118	0.381	0.131	<u>0.059</u>	0.111	<b>0.055</b>
	MSE	<u>0.052</u>	0.052	0.140	0.120	0.155	0.114	0.882	0.133	<u>0.052</u>	0.081	<b>0.048</b>
Exchange	MAE	0.088	0.108	0.187	0.125	0.216	0.091	0.626	0.401	<u>0.056</u>	0.115	<b>0.034</b>
	MSE	0.025	0.031	0.082	0.065	0.124	0.052	1.109	0.337	<u>0.007</u>	0.036	<b>0.003</b>
BeijingAir	MAE	<u>0.358</u>	0.371	0.382	0.368	0.405	0.381	0.543	0.441	0.366	0.376	<b>0.348</b>
	MSE	<b>0.532</b>	0.587	0.598	0.568	0.619	0.592	1.018	0.691	0.564	0.585	<u>0.533</u>

where  $\alpha, \beta, \gamma \in \mathbb{R}$  are the preset balancing coefficients. This entire guidance helps CRIB extract the most important task-relevant information from the partially observed data while filtering out noise introduced by missing values.

## 4. Experiment

### 4.1. Experiment Settings

**Datasets.** We evaluate our model on 11 MTSF datasets: PEMS-BAY, Metr-LA (Li et al., 2017), ETTh1, ETTh2, ETTm1, ETTm2 (Zhou et al., 2021), Weather (Miao et al., 2024), BeijingAir, Exchange (Lai et al., 2018), Electricity (Wu et al., 2021), and AQI (Yi et al., 2016). More information about these datasets is summarized in App. C.

**Baselines.** We evaluate 16 representative baselines: (1) MTSF-M methods: BRITS (Cao et al., 2018), SAITS (Du et al., 2023), SPIN (Marisca et al., 2022), GRIN (Cini et al., 2021), and BiTGraph (Chen et al., 2023). (2) Imputation methods: CSDI (Tashiro et al., 2021), NeuralCDE (Kidger et al., 2020), ImputeFormer (Nie et al., 2024), and TimesNet (Wu et al., 2022). (3) Transformer-based MTSF methods: iTransformer (Liu et al., 2023), PatchTST (Nie et al., 2022), and PAtn (Tan et al., 2024). (4) MLP- and RNN-based MTSF methods: DLinear (Zeng et al., 2023), WP-Mixer (Murad et al., 2025), TimeXer (Wang et al., 2024a), and SegRNN (Lin et al., 2023).

**Implementation Details.** Several forecasting baselines are not originally designed for MTSF-M settings. We therefore construct two-stage variants by combining them with SOTA imputation model **TimesNet** (Wu et al., 2022), which imputes missing values before forecasting. To simulate a practical scenario where ground truth for missing values is unavailable during inference, TimesNet is trained with a 10% missing rate and then used to impute datasets with 20%, 40%, 60%, and 70% missing rates. The original models and the variants are denoted as **Original** and **Imputed**, respectively. More details are provided in App. D.1.

**Training.** We evaluate forecasting performance using Mean Squared Error (MSE) and Mean Absolute Error (MAE). Our training cost is in App. D.3.

### 4.2. Main Results

The average performance comparisons are reported in Tabs. 1 and 2, with full results and additional missing-pattern evaluations provided in App. H and Figure 3. We denote out-of-memory and improvement as OOM and IMP, respectively. Based on these results, we summarize our observations (**Obs.**) as follows:

**Obs. ①: CRIB demonstrates superior performance improvement in MTSF-M tasks.** Overall, CRIB consistently improves forecasting accuracy over strong baselines across diverse datasets and missing-value settings. Specifically, CRIB reduces the MAE by over 18% on ETTh1 and over 13% on PEMS-BAY compared to the strongest baseline. We attribute this improvement to our model’s design, which integrates patch embedding, unified-variate attention, and consistency regularization under the IB principle, thus enabling CRIB to effectively filter noise from incomplete data while preserving essential predictive signals.

**Obs. ②: Modern MTSF models have surpassed specialized models, and applying imputation to them is often detrimental.** Our experiments show that recent MTSF models (e.g., PatchTST), when applied directly to partially observed data, consistently outperform methods designed

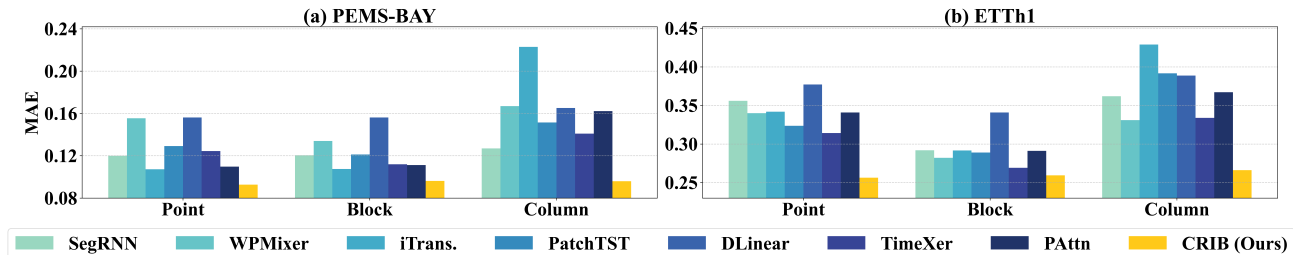


Figure 3. Average MAE on PEMS-BAY and ETTh1 with point, block, and column missing patterns.

specifically for missing values (e.g., BiTGraph). Moreover, we find that applying an explicit imputation step to these modern models is often harmful; their performance on partially observed data is frequently superior to that of their two-stage variants, which use a pre-trained imputer (e.g., TimesNet). For example, PatchTST has an average 0.324 MAE while its variant has a worse average 0.386 MAE on the ETTh1 dataset. These phenomena suggest that imputation without direct ground-truth supervision can introduce erroneous values. This, in turn, distorts the underlying data distribution and corrupts variate correlations, ultimately degrading forecasting performance.

### 4.3. Natural Missingness Evaluation

Table 3. Performance comparison on AQI datasets (Original vs. Imputed). The best results are highlighted in **Bold**, and the second-best is highlighted in Underline.

Data	Metric	SegRNN	WPMixer	iTrans.	PatchTST	DLinear	PAttn	CSDI	NeuralODE	Impute2vec	TimesNet	Ours
AQLORI	MAE	0.604	0.624	0.608	0.627	<b>0.598</b>	0.621	0.858	0.798	0.795	0.648	<b>0.555</b>
	MSE	0.804	0.843	0.818	0.844	<b>0.741</b>	0.843	1.448	1.438	1.313	0.925	<b>0.663</b>
AQLIMP	MAE	<b>0.650</b>	0.665	0.668	0.666	0.653	0.663	0.941	0.946	0.857	0.733	<b>0.616</b>
	MSE	0.966	0.986	1.012	0.993	<b>0.893</b>	0.995	1.775	1.928	1.543	1.206	<b>0.844</b>

**Obs. ③: Imputation-based strategies consistently underperform direct prediction on naturally missing data.**

As shown in Tab. 3, models trained on the fully imputed dataset (AQLIMP) yield higher error rates on observed entries compared to the original sparse data (AQLORI). We attribute this degradation to distributional perturbations introduced by unsupervised imputation. Lacking ground truth, the imputer generates synthetic artifacts that deviate from real dynamics. Consequently, the downstream model is forced to fit these erratic perturbations, which distorts feature representation and impairs its ability to capture authentic dependencies in valid observations. More implementation details are in App. D.2.

### 4.4. Ablation and Sensitivity Study

We further conduct ablation and parameter sensitivity studies on the PEMS-BAY, ETTh1, Electricity and Metr-LA datasets under four missing rates to examine the contribution and robustness of each component in CRIB. In the **Ablation Study** (Figure 4 (a) and App. F), we design three ablation experiments with configurations as follows: (1) **w/o**

**Uni-Atten**: we replace the unified-variate attention mechanism with the vanilla attention mechanism. (2) **w/o Consis**: we remove the consistency regularization. (3) **w/o IB**: we remove the compactness and informativeness guidance of IB. We get observations as follows:

**Obs. ④: Capturing variate correlations and ensuring consistency are critical for direct forecasting.** Removing either the unified-variate attention mechanism or the consistency regularization leads to clear performance degradation across all missing settings. This indicates that explicitly modeling inter-variate correlations and enforcing representation consistency are both essential for accurate forecasting under missingness. Moreover, as shown in Tab. 4, consistency regularization plays an important role in stabilizing training and reducing prediction variance, as reflected by the increased error and instability observed when it is removed.

**Obs. ⑤: The Information Bottleneck principle is the model’s foundational component.** Among all ablation variants, eliminating the IB guidance results in the most severe performance drop. Compared with other components, the IB principle has a more fundamental impact on model behavior, as it directly governs the balance between filtering irrelevant noise and preserving predictive information from incomplete inputs. The sharp degradation of the w/o IB variant, contrasted with the relatively stable performance of other ablations, confirms that IB serves as the core mechanism that enables CRIB to learn robust and compact representations under missing values.

We additionally conduct the **Sensitivity Study** (Figure 4 (b) and App. G) of key hyperparameters, we vary the weights assigned to the **Embedding Size**, **IB weight**:  $\alpha$ , and **Consis Weight**:  $\gamma$  to study how each impacts model performance.

**Obs. ⑥: CRIB is robust to hyperparameter variations, though over-regularization can be detrimental under high missing rates.** As shown in Figure 4 (b), a larger embedding size generally correlates with better performance. However, the model remains effective even with a small embedding size (e.g., 32), demonstrating its efficiency in terms of computational and memory costs. For the IB and consistency regularization weights, we observe a trade-off. At low missing rates, higher weight values can improve ac-

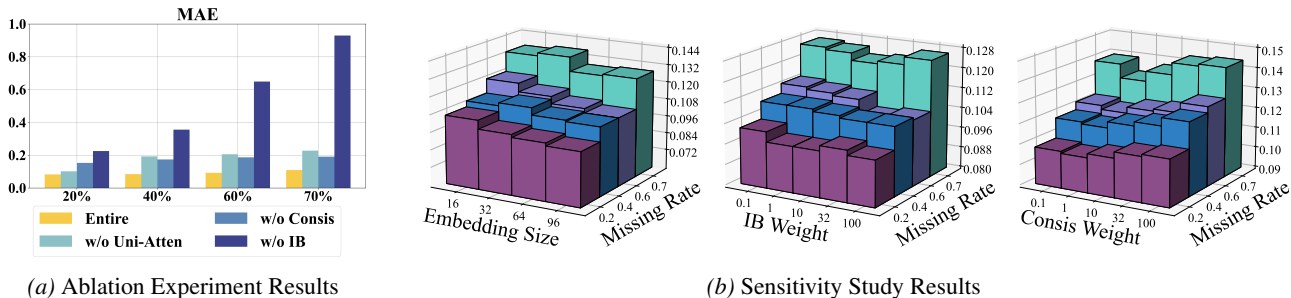


Figure 4. Ablation and Sensitivity experiment results on PEMS-BAY dataset of CRIB.

Table 4. Ablation study of consistency regularization under different missing rates on ETTh1.

Method	Missing 20%		Missing 40%		Missing 60%		Missing 70%	
	MAE	MSE	MAE	MSE	MAE	MSE	MAE	MSE
w/o Consis	0.235±0.0022	0.264±0.0001	0.283±0.0011	0.276±0.0003	0.339±0.0021	0.405±0.0003	0.448±0.0020	0.574±0.0010
<b>CRIB</b>	<b>0.220±0.0001</b>	<b>0.171±0.0001</b>	<b>0.251±0.0001</b>	<b>0.249±0.0001</b>	<b>0.267±0.0001</b>	<b>0.296±0.0001</b>	<b>0.288±0.0001</b>	<b>0.361±0.0008</b>

curacy. However, as the missing rate increases, excessively high weights tend to over-regularize the model, which can hinder its ability to capture complex variate correlations and thus degrade the final forecasting performance.

## 5. Related Work

**Multivariate Time Series Forecasting with Missing Values** Existing MTSF methods (Liu et al., 2023; Wang et al., 2024a; Hu et al., 2025d), which typically assume complete data, suffer significant performance degradation when applied to partially observed datasets. To address this issue, research on MTSF-M has emerged, focusing mainly on two directions: two-stage frameworks and end-to-end models. Two-stage methods combine imputation models (Cao et al., 2018; Cini et al., 2021; Marisca et al., 2022) with forecasting models (Liu et al., 2023; Wu et al., 2021; Tashiro et al., 2021). However, this decoupled design often leads to error propagation across stages (Chen et al., 2023), reducing overall forecasting accuracy. End-to-end approaches, on the other hand, aim to jointly impute missing values and perform forecasting by interleaving spatial and temporal modules (Yu et al., 2024). Despite their promise, these methods face a key limitation: the lack of ground truth for the missing values. As a result, the imputation process becomes noisy, which negatively impacts prediction performance. To address these limitations, we propose a direct prediction method CRIB, which integrates an IB-based Consistency Regularization to effectively identify relevant signals while filtering out redundant or noisy information, leading to more accurate forecasts.

**Information Bottleneck for Time Series** The IB principle provides a theoretical framework for learning compact representations that retain maximal task-relevant in-

formation while discarding irrelevant variability (Tishby et al., 2000). In the context of time series modeling, IB is commonly implemented via Variational Autoencoders (VAEs) (Kingma, 2013; Voloshynovskiy et al., 2019). Existing methods like GP-VAE (Fortuin et al., 2020), MTS-IB (Ullmann et al., 2023), and RIB (Xu & Fekri, 2018) use the IB framework to model temporal dynamics. However, these approaches face a key limitation: a direct application of the IB principle can cause the model to concentrate too narrowly on observed features (Choi & Lee, 2023; Zhang et al., 2025b), thereby neglecting the broader variate correlations crucial for forecasting from incomplete data. In contrast to these works, our proposed CRIB applies the IB principle with a unified-attention mechanism and a consistency regularization. This design enables the model to leverage the regularization benefits of IB while avoiding excessive information collapse, resulting in representations that are both compact and robust to sparsity in the inputs.

## 6. Conclusion

In this paper, we analyze the dominant ‘imputation-then-prediction’ paradigm for MTSF-M tasks. Our empirical analysis reveals a fundamental flaw in this framework: without direct supervision, imputation can corrupt data distribution and degrade, rather than improve, final forecasting accuracy. To address this, we propose a direct prediction paradigm and introduce CRIB, a novel framework designed to learn directly from incomplete data. By leveraging the IB principle with unified-variate attention and consistency regularization, CRIB effectively filters noise while capturing robust predictive signals from partial observations. Extensive experiments validate our method, showing that CRIB achieves a significant 18% improvement and confirms the superiority of direct prediction.

## Impact Statement

This paper presents work whose goal is to advance the field of Machine Learning. There are many potential societal consequences of our work, none of which we feel must be specifically highlighted here.

## References

- Alemi, A. A., Fischer, I., Dillon, J. V., and Murphy, K. Deep variational information bottleneck. *arXiv preprint arXiv:1612.00410*, 2016.
- Bachman, P., Alsharif, O., and Precup, D. Learning with pseudo-ensembles. *Advances in neural information processing systems*, 27, 2014.
- Bai, L., Yao, L., Li, C., Wang, X., and Wang, C. Adaptive graph convolutional recurrent network for traffic forecasting. *Advances in neural information processing systems*, 33:17804–17815, 2020.
- Bai, S., Kolter, J. Z., and Koltun, V. An empirical evaluation of generic convolutional and recurrent networks for sequence modeling. *arXiv preprint arXiv:1803.01271*, 2018.
- Cao, D., Wang, Y., Duan, J., Zhang, C., Zhu, X., Huang, C., Tong, Y., Xu, B., Bai, J., Tong, J., et al. Spectral temporal graph neural network for multivariate time-series forecasting. *Advances in neural information processing systems*, 33:17766–17778, 2020.
- Cao, W., Wang, D., Li, J., Zhou, H., Li, L., and Li, Y. Brits: Bidirectional recurrent imputation for time series. *Advances in neural information processing systems*, 31, 2018.
- Chalk, M., Marre, O., and Tkacik, G. Relevant sparse codes with variational information bottleneck. *Advances in Neural Information Processing Systems*, 29, 2016.
- Chen, X., Li, X., Liu, B., and Li, Z. Biased temporal convolution graph network for time series forecasting with missing values. In *The Twelfth International Conference on Learning Representations*, 2023.
- Choi, M. and Lee, C. Conditional information bottleneck approach for time series imputation. In *The Twelfth International Conference on Learning Representations*, 2023.
- Cini, A., Marisca, I., and Alippi, C. Filling the gaps: Multivariate time series imputation by graph neural networks. *arXiv preprint arXiv:2108.00298*, 2021.
- Du, W., Côté, D., and Liu, Y. Saits: Self-attention-based imputation for time series. *Expert Systems with Applications*, 219:119619, 2023.
- Ekambaram, V., Jati, A., Nguyen, N., Sinthong, P., and Kalagnanam, J. Tsmixer: Lightweight mlp-mixer model for multivariate time series forecasting. In *Proceedings of the 29th ACM SIGKDD Conference on Knowledge Discovery and Data Mining*, pp. 459–469, 2023.
- Fortuin, V., Baranchuk, D., Rätsch, G., and Mandt, S. Gpvae: Deep probabilistic time series imputation. In *International conference on artificial intelligence and statistics*, pp. 1651–1661. PMLR, 2020.
- Hu, Y., Li, Y., Liu, P., Zhu, Y., Li, N., Dai, T., tao Xia, S., Cheng, D., and Jiang, C. Fintsb: A comprehensive and practical benchmark for financial time series forecasting. *arXiv preprint arXiv:2502.18834*, 2025a.
- Hu, Y., Liu, P., Li, Y., Cheng, D., Li, N., Dai, T., Bao, J., and Shu-Tao, X. Finmamba: Market-aware graph enhanced multi-level mamba for stock movement prediction. *arXiv preprint arXiv:2502.06707*, 2025b.
- Hu, Y., Liu, P., Zhu, P., Cheng, D., and Dai, T. Adaptive multi-scale decomposition framework for time series forecasting. In *Proceedings of the AAAI Conference on Artificial Intelligence*, volume 39, pp. 17359–17367, 2025c.
- Hu, Y., Yang, J., Zhou, T., Liu, P., Tang, Y., Jin, R., and Sun, L. Bridging past and future: Distribution-aware alignment for time series forecasting. *arXiv preprint arXiv:2509.14181*, 2025d.
- Hu, Y., Zhang, G., Liu, P., Lan, D., Li, N., Cheng, D., Dai, T., Xia, S.-T., and Pan, S. Timefilter: Patch-specific spatial-temporal graph filtration for time series forecasting. In *Forty-second International Conference on Machine Learning*, 2025e.
- Kidger, P., Morrill, J., Foster, J., and Lyons, T. Neural controlled differential equations for irregular time series. *Advances in neural information processing systems*, 33: 6696–6707, 2020.
- Kingma, D. P. Auto-encoding variational bayes. *arXiv preprint arXiv:1312.6114*, 2013.
- Kingma, D. P. Adam: A method for stochastic optimization. *arXiv preprint arXiv:1412.6980*, 2014.
- Lai, G., Chang, W.-C., Yang, Y., and Liu, H. Modeling long-and short-term temporal patterns with deep neural networks. In *The 41st international ACM SIGIR conference on research & development in information retrieval*, pp. 95–104, 2018.
- Laine, S. and Aila, T. Temporal ensembling for semi-supervised learning. *arXiv preprint arXiv:1610.02242*, 2016.

- Li, X., Li, H., Lu, H., Jensen, C. S., Pandey, V., and Markl, V. Missing value imputation for multi-attribute sensor data streams via message propagation. *Proceedings of the VLDB Endowment*, 17(3):345–358, 2023.
- Li, Y., Yu, R., Shahabi, C., and Liu, Y. Diffusion convolutional recurrent neural network: Data-driven traffic forecasting. *arXiv preprint arXiv:1707.01926*, 2017.
- Li, Y., Yang, X., Yang, X., Xu, M., Wang, X., Liu, W., and Bian, J. R&d-agent-quant: A multi-agent framework for data-centric factors and model joint optimization. *arXiv preprint arXiv:2505.15155*, 2025.
- Lin, S., Lin, W., Wu, W., Zhao, F., Mo, R., and Zhang, H. Segrnn: Segment recurrent neural network for long-term time series forecasting. *arXiv preprint arXiv:2308.11200*, 2023.
- Liu, S., Yu, H., Liao, C., Li, J., Lin, W., Liu, A. X., and Dastdar, S. Pyraformer: Low-complexity pyramidal attention for long-range time series modeling and forecasting. In *International Conference on Learning Representations*, 2022.
- Liu, Y., Hu, T., Zhang, H., Wu, H., Wang, S., Ma, L., and Long, M. itransformer: Inverted transformers are effective for time series forecasting. *arXiv preprint arXiv:2310.06625*, 2023.
- Ma, G., Jiang, R., Yan, R., and Tang, H. Temporal conditioning spiking latent variable models of the neural response to natural visual scenes. *Advances in Neural Information Processing Systems*, 36:3819–3840, 2023.
- Marisca, I., Cini, A., and Alippi, C. Learning to reconstruct missing data from spatiotemporal graphs with sparse observations. *Advances in Neural Information Processing Systems*, 35:32069–32082, 2022.
- Miao, H., Zhao, Y., Guo, C., Yang, B., Zheng, K., Huang, F., Xie, J., and Jensen, C. S. A unified replay-based continuous learning framework for spatio-temporal prediction on streaming data. In *2024 IEEE 40th International Conference on Data Engineering (ICDE)*, pp. 1050–1062. IEEE, 2024.
- Murad, M. M. N., Aktukmak, M., and Yilmaz, Y. Wpmixer: Efficient multi-resolution mixing for long-term time series forecasting. In *Proceedings of the AAAI Conference on Artificial Intelligence*, volume 39, pp. 19581–19588, 2025.
- Nie, T., Qin, G., Ma, W., Mei, Y., and Sun, J. Imputeformer: Low rankness-induced transformers for generalizable spatiotemporal imputation. In *Proceedings of the 30th ACM SIGKDD conference on knowledge discovery and data mining*, pp. 2260–2271, 2024.
- Nie, Y., Nguyen, N. H., Sinthong, P., and Kalagnanam, J. A time series is worth 64 words: Long-term forecasting with transformers. *arXiv preprint arXiv:2211.14730*, 2022.
- Peng, J., Yang, M., Zhang, Q., and Li, X. S4m: S4 for multivariate time series forecasting with missing values. *arXiv preprint arXiv:2503.00900*, 2025.
- Schaffer, A. L., Dobbins, T. A., and Pearson, S.-A. Interrupted time series analysis using autoregressive integrated moving average (arima) models: a guide for evaluating large-scale health interventions. *BMC medical research methodology*, 21:1–12, 2021.
- Shang, P., Liu, X., Yu, C., Yan, G., Xiang, Q., and Mi, X. A new ensemble deep graph reinforcement learning network for spatio-temporal traffic volume forecasting in a freeway network. *Digital Signal Processing*, 123:103419, 2022.
- Tan, J., Liu, H., Li, Y., Yin, S., and Yu, C. A new ensemble spatio-temporal pm2.5 prediction method based on graph attention recursive networks and reinforcement learning. *Chaos, Solitons & Fractals*, 162:112405, 2022.
- Tan, M., Merrill, M., Gupta, V., Althoff, T., and Hartvigsen, T. Are language models actually useful for time series forecasting? *Advances in Neural Information Processing Systems*, 37:60162–60191, 2024.
- Tang, X., Yao, H., Sun, Y., Aggarwal, C., Mitra, P., and Wang, S. Joint modeling of local and global temporal dynamics for multivariate time series forecasting with missing values. In *Proceedings of the AAAI conference on artificial intelligence*, volume 34, pp. 5956–5963, 2020.
- Tashiro, Y., Song, J., Song, Y., and Ermon, S. CsdI: Conditional score-based diffusion models for probabilistic time series imputation. *Advances in Neural Information Processing Systems*, 34:24804–24816, 2021.
- Tishby, N. and Zaslavsky, N. Deep learning and the information bottleneck principle. In *2015 IEEE information theory workshop (itw)*, pp. 1–5. IEEE, 2015.
- Tishby, N., Pereira, F. C., and Bialek, W. The information bottleneck method. *arXiv preprint physics/0004057*, 2000.
- Ullmann, D., Taran, O., and Voloshynovskiy, S. Multivariate time series information bottleneck. *Entropy*, 25(5):831, 2023.
- Vaswani, A. Attention is all you need. *Advances in Neural Information Processing Systems*, 2017.
- Voloshynovskiy, S., Kondah, M., Rezaeifar, S., Taran, O., Holotyak, T., and Rezende, D. Information bottleneck

- through variational glasses. *arxiv*. 2019 doi: 10.48550. *arxiv*, 1912.
- Voloshynovskiy, S., Kondah, M., Rezaeifar, S., Taran, O., Holotyak, T., and Rezende, D. J. Information bottleneck through variational glasses. *arXiv preprint arXiv:1912.00830*, 2019.
- Wang, Y., Wu, H., Dong, J., Qin, G., Zhang, H., Liu, Y., Qiu, Y., Wang, J., and Long, M. Timexer: Empowering transformers for time series forecasting with exogenous variables. *Advances in Neural Information Processing Systems*, 37:469–498, 2024a.
- Wang, Y., Xu, Y., Yang, J., Wu, M., Li, X., Xie, L., and Chen, Z. Fully-connected spatial-temporal graph for multivariate time-series data. In *Proceedings of the AAAI Conference on Artificial Intelligence*, volume 38, pp. 15715–15724, 2024b.
- Wen, Q., Sun, L., Yang, F., Song, X., Gao, J., Wang, X., and Xu, H. Time series data augmentation for deep learning: A survey. *arXiv preprint arXiv:2002.12478*, 2020.
- Wu, H., Xu, J., Wang, J., and Long, M. Autoformer: Decomposition transformers with auto-correlation for long-term series forecasting. *Advances in neural information processing systems*, 34:22419–22430, 2021.
- Wu, H., Hu, T., Liu, Y., Zhou, H., Wang, J., and Long, M. Timesnet: Temporal 2d-variation modeling for general time series analysis. *arXiv preprint arXiv:2210.02186*, 2022.
- Wu, S.-F., Chang, C.-Y., and Lee, S.-J. Time series forecasting with missing values. In *2015 1st International Conference on Industrial Networks and Intelligent Systems (INISCom)*, pp. 151–156. IEEE, 2015.
- Xu, D. and Fekri, F. Time series prediction via recurrent neural networks with the information bottleneck principle. In *2018 IEEE 19th International Workshop on Signal Processing Advances in Wireless Communications (SPAWC)*, pp. 1–5. IEEE, 2018.
- Yang, J., Zhang, K., Zhang, G., Yu, P. S., and Ding, K. Glocal information bottleneck for time series imputation. *arXiv preprint arXiv:2510.04910*, 2025.
- Yi, K., Zhang, Q., Fan, W., He, H., Hu, L., Wang, P., An, N., Cao, L., and Niu, Z. Fouriergnn: Rethinking multivariate time series forecasting from a pure graph perspective. *Advances in Neural Information Processing Systems*, 36, 2024.
- Yi, X., Zheng, Y., Zhang, J., and Li, T. St-mvl: Filling missing values in geo-sensory time series data. In *Proceedings of the 25th international joint conference on artificial intelligence*, 2016.
- Yu, B., Yin, H., and Zhu, Z. Spatio-temporal graph convolutional networks: A deep learning framework for traffic forecasting. *arXiv preprint arXiv:1709.04875*, 2017.
- Yu, C., Wang, F., Shao, Z., Qian, T., Zhang, Z., Wei, W., and Xu, Y. Ginar: An end-to-end multivariate time series forecasting model suitable for variable missing. In *Proceedings of the 30th ACM SIGKDD Conference on Knowledge Discovery and Data Mining*, pp. 3989–4000, 2024.
- Yu, C., Wang, F., Shao, Z., Qian, T., Zhang, Z., Wei, W., An, Z., Wang, Q., and Xu, Y. Ginar+: A robust end-to-end framework for multivariate time series forecasting with missing values. *IEEE Transactions on Knowledge and Data Engineering*, 2025.
- Zeng, A., Chen, M., Zhang, L., and Xu, Q. Are transformers effective for time series forecasting? In *Proceedings of the AAAI conference on artificial intelligence*, volume 37, pp. 11121–11128, 2023.
- Zhang, K., Jing, B., Candan, K. S., Zhou, D., Wen, Q., Liu, H., and Ding, K. Cross-domain conditional diffusion models for time series imputation. *arXiv preprint arXiv:2506.12412*, 2025a.
- Zhang, S., Wang, J., Nie, S., Yue, J., Zhu, W., and Lin, Y. Loss or gain: Hierarchical conditional information bottleneck approach for incomplete time series classification. In *Proceedings of the 31st ACM SIGKDD Conference on Knowledge Discovery and Data Mining V. 2*, pp. 3796–3807, 2025b.
- Zheng, Y., Yi, X., Li, M., Li, R., Shan, Z., Chang, E., and Li, T. Forecasting fine-grained air quality based on big data. In *Proceedings of the 21th ACM SIGKDD international conference on knowledge discovery and data mining*, pp. 2267–2276, 2015.
- Zhou, F., Pan, C., Ma, L., Liu, Y., Wang, S., Zhang, J., Zhu, X., Hu, X., Hu, Y., Zheng, Y., et al. Sloth: structured learning and task-based optimization for time series forecasting on hierarchies. In *Proceedings of the AAAI Conference on Artificial Intelligence*, volume 37, pp. 11417–11425, 2023.
- Zhou, H., Zhang, S., Peng, J., Zhang, S., Li, J., Xiong, H., and Zhang, W. Informer: Beyond efficient transformer for long sequence time-series forecasting. In *Proceedings of the AAAI conference on artificial intelligence*, volume 35, pp. 11106–11115, 2021.
- Zhu, P., Li, Y., Hu, Y., Liu, Q., Cheng, D., and Liang, Y. Lsr-igr: Stock trend prediction based on long short-term relationships and improved gru. In *Proceedings of the 33rd ACM International Conference on Information and Knowledge Management*, pp. 5135–5142, 2024.

Zuo, J., Zeitouni, K., Taher, Y., and Garcia-Rodriguez, S.  
Graph convolutional networks for traffic forecasting with  
missing values. *Data Mining and Knowledge Discovery*,  
37(2):913–947, 2023.

## A. Full Derivation

We illustrate the full derivation of the two terms of IB as follows.

### Compactness Principle:

$$\begin{aligned}
 I_\theta(Z; X^o) &= \mathbb{E}_{p(x^o, z)} \left[ \log \frac{p(x^o, z)}{p(z) \cdot p(x^o)} \right], \\
 &= \mathbb{E}_{p(x^o, z)} \left[ \log \frac{p(z|x^o) \cdot p(x^o)}{p(z) \cdot p(x^o)} \right], \\
 &= \mathbb{E}_{p(x^o, z)} \left[ \log \frac{p(z|x^o)}{p(z)} \right], \\
 &= \mathbb{E}_{p(x^o, z)} \left[ \log \frac{p(z|x^o)}{p(z)} \cdot \frac{q(z)}{q(z)} \right], \\
 &= \mathbb{E}_{p(x^o, z)} \left[ \log \frac{p(z|x^o)}{q(z)} \right] - \mathbb{E}_{p(x^o, z)} \left[ \log \frac{p(z)}{q(z)} \right], \\
 &= \mathbb{E}_{p(x^o, z)} \left[ \log \frac{p(z|x^o)}{q(z)} \right] - D_{KL}[p(z) || q(z)], \\
 &= \mathbb{E}_{p(x^o)} [D_{KL}(p(z|x^o) || q(z))] - D_{KL}[p(z) || q(z)], \\
 &\leq \mathbb{E}_{p(x^o)} [D_{KL}(p(z|x^o) || p(z))].
 \end{aligned} \tag{13}$$

### Informativeness Principle:

$$\begin{aligned}
 I_\theta(Y; Z) &= \mathbb{E}_{p(z, y)} \left[ \log \frac{p(z, y)}{p(z) \cdot p(y)} \right], \\
 &= \mathbb{E}_{p(z, y)} \left[ \log \frac{p(y|z) \cdot p(z)}{p(y) \cdot p(z)} \right], \\
 &= \mathbb{E}_{p(z, y)} \left[ \log \frac{p(y|z)}{p(y)} \right], \\
 &= \mathbb{E}_{p(z, y)} \left[ \log \frac{p(y|z) \cdot q_\theta(y|z)}{p(y) \cdot q_\theta(y|z)} \right], \\
 &= \mathbb{E}_{p(z, y)} \left[ \log \frac{q_\theta(y|z)}{p(y)} \right] + \mathbb{E}_{p(z, y)} \left[ \log \frac{p(y|z)}{q_\theta(y|z)} \right], \\
 &= \mathbb{E}_{p(z, y)} \left[ \log \frac{q_\theta(y|z)}{p(y)} \right] + \iint_{z, y} p(z) \cdot p(y|z) \cdot \log \frac{p(y|z)}{q_\theta(y|z)} dz dy, \\
 &= \mathbb{E}_{p(z, y)} \left[ \log \frac{q_\theta(y|z)}{p(y)} \right] + \int_z p(z) \cdot D_{KL}[p(y|z) || q_\theta(y|z)] dz \\
 &\geq \mathbb{E}_{p(z, y)} \left[ \log \frac{q_\theta(y|z)}{p(y)} \right], \\
 &= \mathbb{E}_{p(z, y)} [\log q_\theta(y|z)] + H(Y), \\
 &\geq \mathbb{E}_{p(z, y)} [\log q_\theta(y|z)].
 \end{aligned} \tag{14}$$

The inequalities of the upper and lower bound in Equations (13) and (14) follow directly from the non-negativity of the KL-divergence and Entropy.

## B. Quantitative Analysis of Introduction

- Detrimental Imputation:** We demonstrate that imputation without ground truth is often harmful. As visualized in Figure 1, methods following the “imputation-then-prediction” paradigm fail to recover the true data distribution and instead reinforce biased patterns from partial observations.

Table 5. Performance comparison on PEMS-BAY dataset (40% Missing).

Metric	CRIB	BiTGraph	DLinear	TimesNet + DLinear	TimeXer	TimesNet + TimeXer
MAE	<b>0.093</b>	0.413	0.156	0.148	<u>0.125</u>	0.135
MSE	<b>0.043</b>	0.788	0.087	0.081	<u>0.051</u>	0.073

- ⊗ **Performance Degradation:** We provide counter-intuitive evidence that imputation actively harms prediction accuracy. For instance, equipping the predictor TimeXer with the SOTA imputer TimesNet increases the MAE from 0.125 to 0.135 as shown in Tab. 5. It also has no help in understanding the data distribution and variate correlations as demonstrated in Figure 1.

## C. Datasets

To assess the model’s effectiveness and robustness in handling missing values, we introduce synthetic missingness by randomly removing data points at varying missing rates of 20%, 40%, 60%, and 70% with three different missing patterns. During the experiments, we normalized the data to facilitate better model fitting.

We introduce information about datasets in Tab. 6.

Table 6. Statistics of the 11 real-world datasets used in our experiments.

Statistics	ETTh1	ETTh2	ETTm1	ETTm2	Electricity	PEMS-BAY	Metr-LA	BeijingAir	Weather	Exchange	AQI
<b>Time Steps</b>	17,420	17,420	69,680	69,680	26,304	52,116	34,272	36,000	52,696	7,588	8759
<b>Variates</b>	7	7	7	7	321	325	207	7	21	8	36

## D. Implementation Details

### D.1. Comparison Evaluations

We use Adam optimizer (Kingma, 2014) to learn the parameters of all models with  $10^{-3}$  learning rate. The unified-variate attention of CRIB is configured with 2 layers and 4 heads, while the predictor is implemented as a simple 2-layer MLP. Both historical and future time window sizes are set to 24 for all methods, following the setting of BiTGraph (Chen et al., 2023). The patch length is set to 8, so every time series in a time window is patched into three tokens. The entire dataset is divided into training, validation, and testing sets with ratios of 60%, 20%, and 20%. All methods are trained on an Nvidia 4090 GPU with PyTorch 2.0. Hyperparameters of all baselines are consistent with their original papers.

### D.2. Natural Missingness Evaluations

To fairly compare direct prediction with the imputation-then-prediction paradigm, we first pre-trained TimesNet (Wu et al., 2022) on the AQI training set for imputation by applying an additional 10% point-missing mask on observed entries, matching the dataset’s estimated natural missing rate. We then used the trained TimesNet to impute all NaNs in AQI and trained/evaluated downstream forecasting models on this fully imputed dataset (AQI\_IMP). In contrast, we trained/evaluated the same models directly on the original AQI with natural missingness (AQI\_ORI).

### D.3. Training Cost

To ensure fair comparisons, we train all baseline models from scratch using identical dataset splits and experimental protocols, as detailed in Sec. 4.1. We evaluate computational efficiency by reporting the memory footprint and parameter counts of every model on ETTh1 as follows.

**Conclusion:** The results demonstrate that CRIB maintains a computational cost comparable to efficient Transformer baselines (e.g., PatchTST (Nie et al., 2022)) while being more lightweight than complex methods such as CSDI (Tashiro et al., 2021) and TimesNet (Wu et al., 2022).

Table 7. Comparison of model efficiency in terms of parameter count and memory cost. CRIB achieves a balanced trade-off between performance and efficiency.

Model	Parameters	Memory (MB)
<b>CRIB (Ours)</b>	<b>37,450</b>	<b>148.03</b>
DLinear	1,200	18.99
PAttn	15,640	55.13
SegRNN	8,056	30.17
Transformer	57,063	189.38
iTransformer	39,768	154.18
PatchTST	41,528	179.80
TSMixer	6,837	21.16
WPMixer	44,370	50.16
CSDI	239,649	1,269.72
NeuralCDE	37,767	41.40
ImputeFormer	264,193	1,488.22
TimesNet	863,895	1,427.44

## E. Extra Experiments

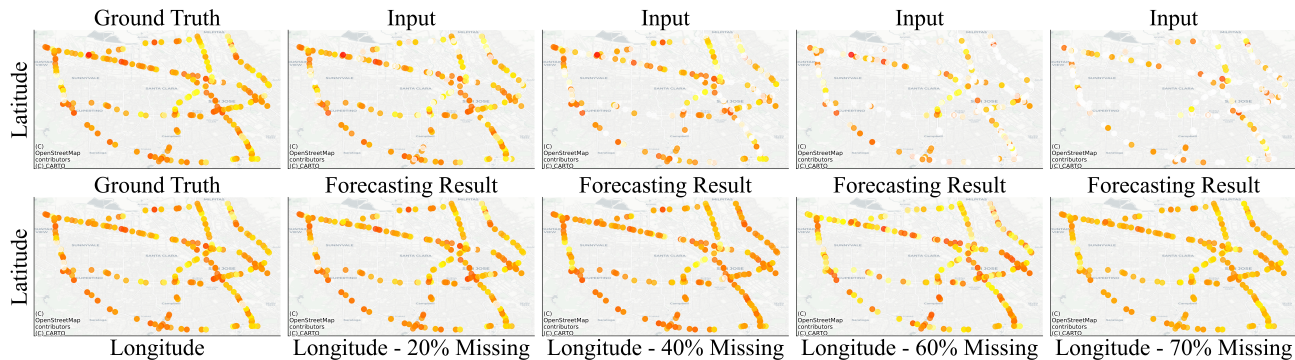


Figure 5. Visualization of the input and forecasting results of CRIB on the PEMS-BAY dataset with missing rates from 20% to 70%.

### E.1. Forecasting Results Visualization

We present a spatial visualization of forecasting results to demonstrate the effectiveness of CRIB under varying missing rates. Figure 5 shows the final timestamp in the historical time window and the first forecasting timestamp on the PEMS-BAY dataset. At lower missing rates (20% and 40%), by effectively leveraging inter-variate correlations extracted from the data, CRIB accurately predicts the future values. Even at higher missing rates (60% and 70%), CRIB can maintain stable performance and predict the spatial distribution of the PEMS-BAY datasets. These findings underscore CRIB’s capability to handle incomplete data and produce reliable predictions.

### E.2. Unified-Variate Attention Maps Visualization

In Figure 6, we compare visualizations of directly applying IB on the Transformer with our proposed CRIB. In the first experiment, a transformer model serves as the predictor. The **left** two figures clearly show that directly applying IB to the model would force the model to focus on a few specific values (straight line attention), thereby neglecting global information. In contrast, the **right** figures reveal that CRIB can not only capture the original intra-variate temporal correlations in one attention head but also effectively uncovers cross-variate correlations in another, rather than relying solely on raw correlations.

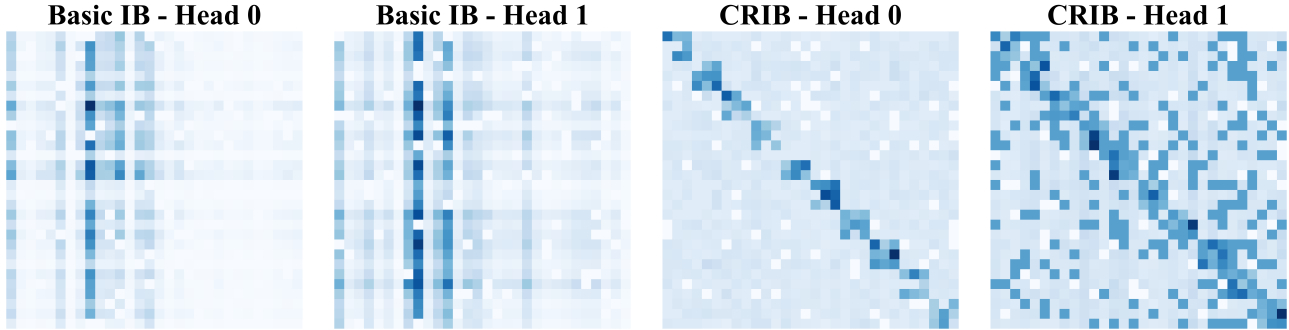


Figure 6. Visualization comparison of attention maps on the Metr-LA dataset with 60% missing values. **Left:** Two attention maps of the direct application of IB on the standard Transformer. **Right:** Two attention maps of CRIB.

As a result, the final forecasting performance is improved remarkably by our unified-variate attention mechanism and consistency regularization scheme.

### E.3. Experiments on Various Missing Patterns

Figures 7 to 14 present the main forecasting results, comparing our proposed model, CRIB, against state-of-the-art baselines. The results clearly show that CRIB consistently achieves the lowest MAE and MSE across all evaluated scenarios. This superiority holds true for both the PEMS-BAY and ETTh1 datasets, under point, block, and column missing patterns, and across a wide range of missing rates from 20% to 70%. Notably, while the performance of most baseline models degrades significantly as the missing rate increases, CRIB maintains its superior performance and stability. This demonstrates the robustness and effectiveness of our direct-prediction approach, validating its superiority over existing methods, especially in challenging high-missing-rate environments.

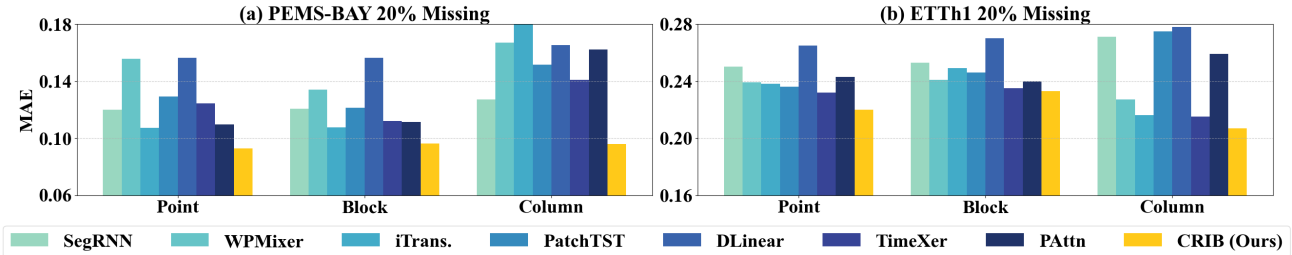


Figure 7. MAE comparison on PEMS-BAY and ETTh1 with point, block, and column missing patterns on 20% missing rate.

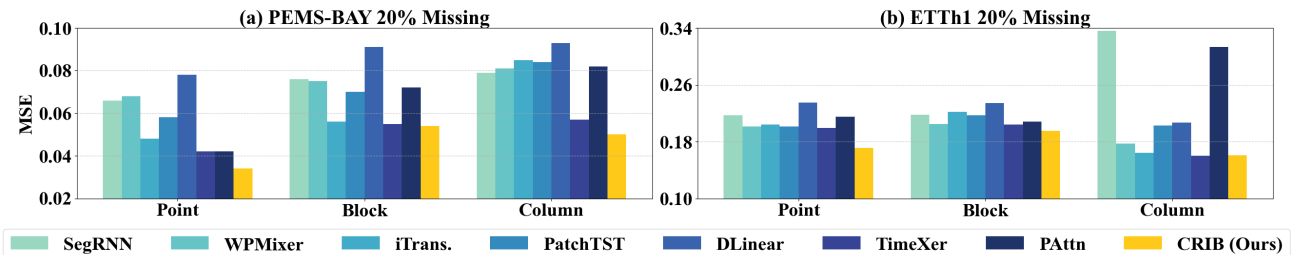


Figure 8. MSE comparison on PEMS-BAY and ETTh1 with point, block, and column missing patterns on 20% missing rate.

### F. Extra Ablation Study

We have done an extra ablation study on three cases of loss of CRIB to prove its effectiveness. The ablation analysis across four datasets confirms the necessity of each component, as removing the Consistency Regularization ( $\mathcal{L}_{\text{Consis}}$ ), Compactness ( $\mathcal{L}_{\text{Comp}}$ ), or Informativeness ( $\mathcal{L}_{\text{Pred}}$ ) objectives consistently leads to performance degradation, validating their collective role in ensuring robust and accurate forecasting in MTSF-M tasks.

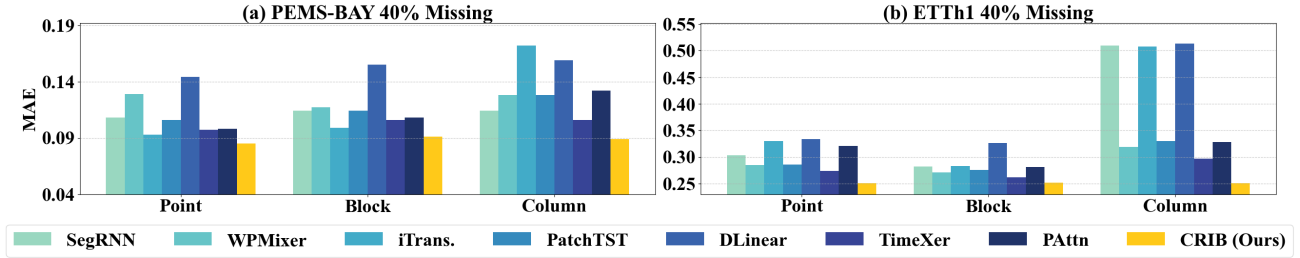


Figure 9. MAE comparison on PEMS-BAY and ETTh1 with point, block, and column missing patterns on 40% missing rate.

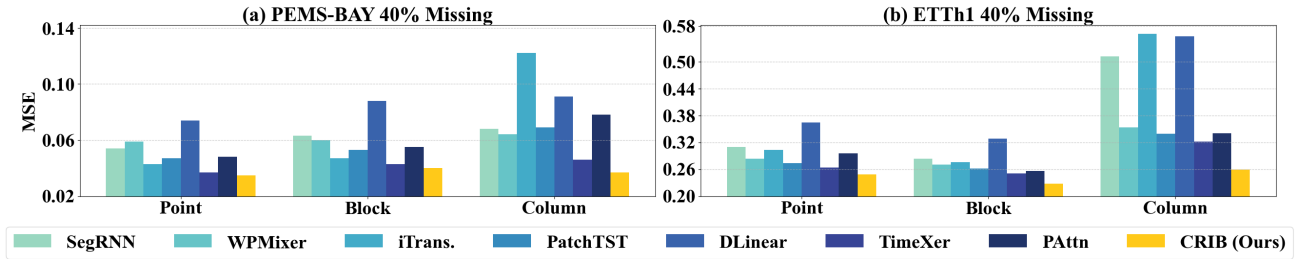


Figure 10. MSE comparison on PEMS-BAY and ETTh1 with point, block, and column missing patterns on 40% missing rate.

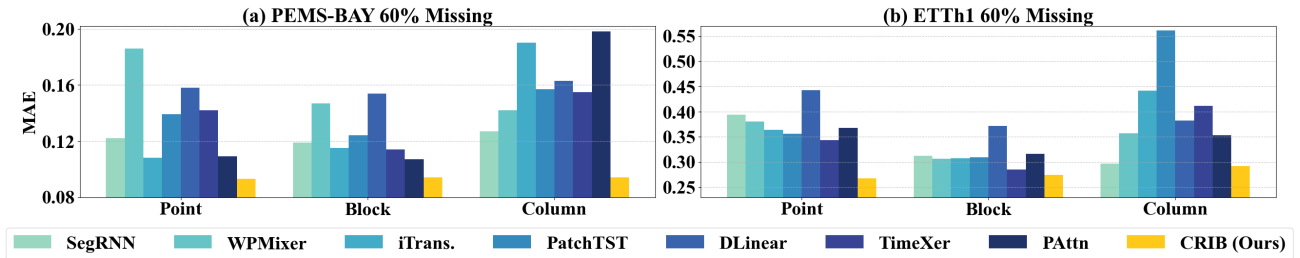


Figure 11. MAE comparison on PEMS-BAY and ETTh1 with point, block, and column missing patterns on 60% missing rate.

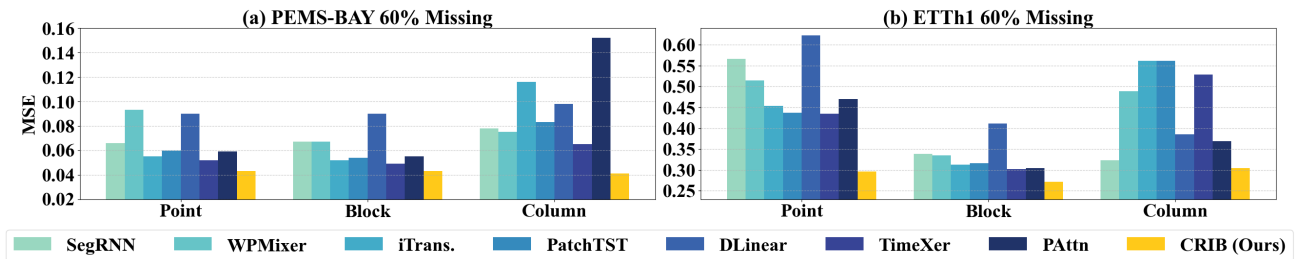


Figure 12. MSE comparison on PEMS-BAY and ETTh1 with point, block, and column missing patterns on 60% missing rate.

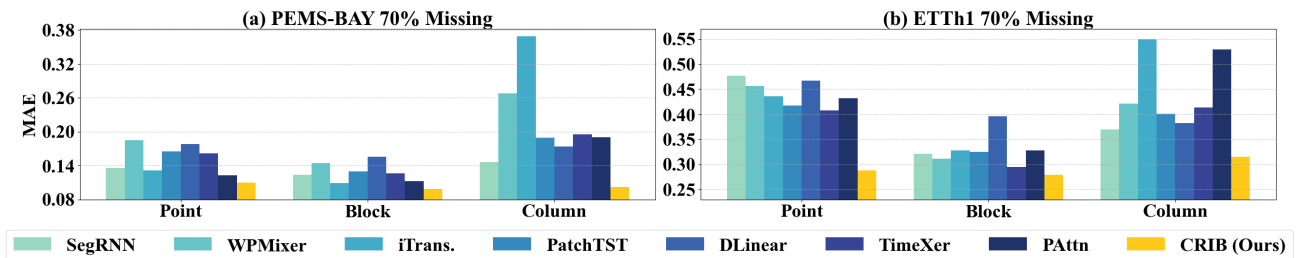


Figure 13. MAE comparison on PEMS-BAY and ETTh1 with point, block, and column missing patterns on 70% missing rate.

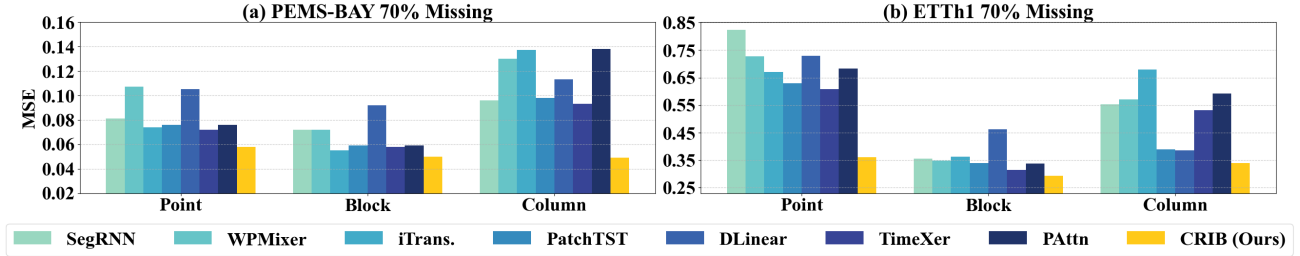


Figure 14. MSE comparison on PEMS-BAY and ETTh1 with point, block, and column missing patterns on 70% missing rate.

Table 8. Ablation study on ETTh1 dataset.

ETTh1	0.2		0.4		0.6		0.7	
	MAE	MSE	MAE	MSE	MAE	MSE	MAE	MSE
w/o Consis	0.237	0.206	0.274	0.270	0.338	0.413	0.402	0.584
w/o Reg	0.236	0.206	0.274	0.270	0.339	0.410	0.400	0.579
w/o Pred	0.432	0.559	0.505	0.698	0.655	1.066	0.796	1.486
<b>Entire</b>	<b>0.220</b>	<b>0.171</b>	<b>0.251</b>	<b>0.249</b>	<b>0.267</b>	<b>0.296</b>	<b>0.288</b>	<b>0.361</b>

Table 9. Ablation study on Elec dataset.

Elec	0.2		0.4		0.6		0.7	
	MAE	MSE	MAE	MSE	MAE	MSE	MAE	MSE
w/o Consis	0.0201	0.0196	0.0267	0.0338	0.0346	0.0569	0.0415	0.0931
w/o Reg	0.0186	0.0175	0.0244	0.0286	0.0322	0.0544	0.0399	0.0980
w/o Pred	0.0881	0.5454	0.1243	0.9424	0.1818	1.8995	0.2283	2.9058
<b>Entire</b>	<b>0.0150</b>	<b>0.0120</b>	<b>0.0230</b>	<b>0.0280</b>	<b>0.0300</b>	<b>0.0470</b>	<b>0.0380</b>	<b>0.0910</b>

Table 10. Ablation study on Metr-LA dataset.

Metr-LA	0.2		0.4		0.6		0.7	
	MAE	MSE	MAE	MSE	MAE	MSE	MAE	MSE
w/o Consis	0.271	0.332	0.257	0.275	0.271	0.306	0.314	0.366
w/o Reg	0.253	0.307	0.251	0.275	0.266	0.307	0.311	0.364
w/o Pred	0.442	0.418	0.624	0.529	0.985	1.177	1.276	1.959
<b>Entire</b>	<b>0.248</b>	<b>0.271</b>	<b>0.249</b>	<b>0.272</b>	<b>0.265</b>	<b>0.305</b>	<b>0.309</b>	<b>0.356</b>

## G. Extra Sensitivity Study

We analyze hyperparameter sensitivity in Figure 4 (b) and conduct additional sensitivity studies. Empirical results indicate that the optimal settings are consistent across different datasets and missing rates. We set the weights for  $\mathcal{L}_{\text{Comp}}$ ,  $\mathcal{L}_{\text{Pred}}$ , and  $\mathcal{L}_{\text{Consis}}$  to  $10^{-6}$ , 1, and 1 as default, respectively.

## H. Full Experiments

Table 11. Ablation study on PEMS-BAY dataset.

PEMS-BAY	0.2		0.4		0.6		0.7	
	MAE	MSE	MAE	MSE	MAE	MSE	MAE	MSE
w/o Consis	0.0959	0.0470	0.0882	0.0389	0.0976	0.0465	0.1296	0.0596
w/o Reg	0.0942	0.0453	0.0869	0.0373	0.0964	0.0456	0.1190	0.0591
w/o Pred	0.4006	0.2405	0.5618	0.3631	1.0832	1.2727	2.1480	4.8111
<b>Entire</b>	<b>0.0830</b>	<b>0.0340</b>	<b>0.0850</b>	<b>0.0350</b>	<b>0.0930</b>	<b>0.0430</b>	<b>0.1100</b>	<b>0.0580</b>

 Table 12. Sensitivity analysis of  $\mathcal{L}_{\text{Pred}}$  weight across all missing rates.

Weight	0% Missing		20% Missing		40% Missing		60% Missing		70% Missing	
	ETTh1	Exchange	ETTh1	Exchange	ETTh1	Exchange	ETTh1	Exchange	ETTh1	Exchange
0.1	0.201	0.0186	0.243	0.0332	0.281	0.0439	0.348	0.0413	0.412	0.0373
0.5	0.198	0.0186	0.238	0.0301	0.273	0.0294	0.340	0.0362	0.406	0.0423
1.0	0.198	0.0186	0.237	0.0287	0.274	0.0253	0.337	0.0363	0.403	0.0517
2.0	0.199	0.0186	0.236	0.0261	0.273	0.0261	0.339	0.0363	0.400	0.0475
5.0	0.200	0.0186	0.237	0.0246	0.273	0.0258	0.338	0.0287	0.401	0.0320

 Table 13. Sensitivity analysis of  $\mathcal{L}_{\text{Comp}}$  weight across all missing rates.

Weight	0% Missing		20% Missing		40% Missing		60% Missing		70% Missing	
	ETTh1	Exchange	ETTh1	Exchange	ETTh1	Exchange	ETTh1	Exchange	ETTh1	Exchange
10	0.214	0.0192	0.260	0.0509	0.314	0.0806	0.417	0.2131	0.506	0.2851
1	0.208	0.0188	0.251	0.0471	0.296	0.0835	0.365	0.1393	0.437	0.2293
$10^{-2}$	0.199	0.0186	0.238	0.0300	0.274	0.0319	0.341	0.0435	0.406	0.0499
$10^{-6}$	0.198	0.0186	0.237	0.0287	0.274	0.0253	0.337	0.0363	0.403	0.0517
$10^{-10}$	0.199	0.0186	0.237	0.0276	0.273	0.0260	0.339	0.0417	0.403	0.0408

 Table 14. Sensitivity analysis of  $\mathcal{L}_{\text{Consis}}$  weight across all missing rates.

Weight	0% Missing		20% Missing		40% Missing		60% Missing		70% Missing	
	ETTh1	Exchange	ETTh1	Exchange	ETTh1	Exchange	ETTh1	Exchange	ETTh1	Exchange
0.1	0.201	0.0186	0.237	0.0231	0.274	0.0270	0.340	0.0301	0.400	0.0341
0.5	0.199	0.0186	0.236	0.0260	0.274	0.0273	0.339	0.0378	0.401	0.0368
1.0	0.198	0.0186	0.237	0.0287	0.274	0.0253	0.337	0.0363	0.403	0.0517
2.0	0.199	0.0186	0.239	0.0306	0.275	0.0300	0.340	0.0352	0.404	0.0427
5.0	0.200	0.0186	0.240	0.0312	0.278	0.0377	0.344	0.0376	0.410	0.0357

Revisiting Multivariate Time Series Forecasting with Missing Values

Table 15. Performance comparison of different models for multivariate time series forecasting with missing values. Missing rate is set at 20%, 40%, 60%, and 70%. The best results are highlighted in **Bold** and the second-best is highlighted in Underline.

Data	Metric	BiTGraph	BRITS	GRIN	SAITS	SPIN	SegRNN		WPMixer		iTransformer		PatchTST		DLinear		TimeXer		PAttn	Ours	
		Original	Original	Imputed	Original	Imputed	Original	Imputed	Original	Imputed	Original	Imputed	Original	Imputed	Original	Imputed	Original	Imputed	Original	Imputed	
PEMS-BAY	MAE@20%	0.403	0.351	0.343	OOM	0.218	0.114	0.231	0.122	0.249	<u>0.097</u>	0.153	0.107	0.158	0.145	0.163	<u>0.097</u>	0.146	0.109	0.173	<b>0.083</b>
	MSE@20%	0.754	0.664	0.585	OOM	0.234	0.066	0.232	0.068	0.193	0.048	0.094	0.058	0.107	0.078	0.096	<u>0.042</u>	0.087	0.062	0.111	<b>0.034</b>
	MAE@40%	0.411	0.360	0.346	OOM	0.288	0.108	0.179	0.129	0.203	<u>0.093</u>	0.127	0.106	0.142	0.144	0.138	0.097	0.140	0.098	0.165	<b>0.085</b>
	MSE@40%	0.777	0.696	0.609	OOM	0.360	0.054	0.185	0.059	0.135	0.043	0.074	0.047	0.087	0.074	0.069	<u>0.037</u>	0.073	0.048	0.100	<b>0.035</b>
	MAE@60%	0.419	0.372	0.355	OOM	0.501	0.122	0.153	0.186	0.181	<u>0.108</u>	0.107	0.139	0.122	0.158	0.141	0.142	0.121	0.109	0.121	<b>0.093</b>
	MSE@60%	0.806	0.720	0.647	OOM	0.948	0.066	0.187	0.093	0.118	0.055	0.060	0.060	0.072	0.090	0.073	<u>0.052</u>	0.061	0.059	0.073	<b>0.043</b>
	MAE@70%	0.420	0.382	0.356	OOM	0.601	0.136	0.148	0.185	0.173	0.131	0.114	0.165	0.134	0.178	0.152	0.162	0.134	<u>0.123</u>	0.131	<b>0.110</b>
	MSE@70%	0.816	0.742	0.653	OOM	1.053	0.081	0.208	0.107	0.116	0.074	0.061	0.076	0.079	0.105	0.084	<u>0.072</u>	0.071	0.076	0.081	<b>0.058</b>
Metri-LA	MAE@20%	0.435	0.351	0.387	0.484	0.336	0.280	0.356	0.300	0.372	<u>0.256</u>	0.308	0.265	0.323	0.319	0.372	0.296	0.306	0.268	0.324	<b>0.248</b>
	MSE@20%	0.760	0.596	0.638	0.743	0.576	0.319	0.406	0.320	0.434	0.309	0.347	0.313	0.374	0.327	0.371	<u>0.303</u>	0.345	0.323	0.370	<b>0.271</b>
	MAE@40%	0.442	0.359	0.390	0.463	0.452	0.317	0.306	0.335	0.334	<u>0.254</u>	0.280	0.302	0.307	0.346	0.344	0.293	0.291	0.308	0.282	<b>0.249</b>
	MSE@40%	0.756	0.600	0.667	0.697	0.692	0.305	0.321	0.301	0.349	<u>0.273</u>	0.297	0.286	0.321	0.299	0.315	<u>0.273</u>	0.306	0.305	0.308	<b>0.272</b>
	MAE@60%	0.449	0.371	0.386	0.434	0.856	0.324	0.293	0.377	0.327	<u>0.274</u>	0.280	0.341	0.296	0.426	0.360	0.327	0.295	0.309	0.277	<b>0.265</b>
	MSE@60%	0.760	0.615	0.649	0.719	1.196	0.326	0.334	0.357	0.357	0.309	0.314	<u>0.308</u>	0.332	0.381	0.351	0.309	0.323	0.316	0.329	<b>0.305</b>
	MAE@70%	0.452	0.382	0.393	0.422	0.856	0.351	0.301	0.411	0.334	<u>0.307</u>	0.291	0.345	0.297	0.506	0.388	0.371	0.299	0.323	0.293	<b>0.309</b>
	MSE@70%	0.765	0.632	0.658	0.723	1.397	0.429	0.380	0.446	0.401	0.378	0.361	0.372	0.370	0.485	0.411	0.369	0.359	0.405	0.371	<b>0.356</b>
ETTh1	MAE@20%	0.257	<u>0.232</u>	0.234	0.369	0.232	0.250	0.394	0.239	0.386	0.238	0.417	0.236	0.398	0.265	0.538	<u>0.232</u>	0.341	0.243	0.432	<b>0.220</b>
	MSE@20%	0.307	0.378	0.282	0.457	<u>0.191</u>	0.217	0.331	0.201	0.323	0.204	0.374	0.201	0.382	0.235	0.508	0.199	0.296	0.215	0.387	<b>0.171</b>
	MAE@40%	0.278	0.317	0.338	0.349	0.320	0.303	0.403	0.285	0.383	0.330	0.493	0.286	0.419	0.334	0.616	<u>0.274</u>	0.340	0.321	0.506	<b>0.251</b>
	MSE@40%	0.316	0.373	0.386	0.430	0.346	0.310	0.384	0.284	0.352	0.303	0.556	0.274	0.445	0.365	0.646	<u>0.264</u>	0.323	0.296	0.518	<b>0.249</b>
	MAE@60%	0.394	0.432	0.399	0.380	0.598	0.394	0.445	0.380	0.404	0.364	0.382	0.356	0.355	0.443	0.631	<u>0.343</u>	0.346	0.368	0.399	<b>0.267</b>
	MSE@60%	0.493	0.499	0.498	0.482	0.667	0.566	0.539	0.514	0.451	0.454	0.454	0.437	0.418	0.623	0.763	<u>0.435</u>	0.393	0.470	0.462	<b>0.296</b>
	MAE@70%	0.420	0.449	0.455	<u>0.390</u>	0.599	0.477	0.459	0.456	0.424	0.436	0.384	0.417	0.373	0.567	0.608	0.408	0.363	0.432	0.390	<b>0.288</b>
	MSE@70%	0.432	0.436	0.433	<u>0.461</u>	0.669	0.824	0.653	0.728	0.541	0.671	0.507	0.630	0.497	1.016	0.812	0.608	0.468	0.683	0.514	<b>0.361</b>
Electricity	MAE@20%	0.029	<u>0.018</u>	0.020	0.050	0.021	0.051	0.357	0.026	0.348	0.020	0.172	0.020	0.143	0.039	0.169	0.019	0.129	0.022	0.197	<b>0.015</b>
	MSE@20%	0.123	0.026	0.015	0.243	0.028	0.478	0.976	0.035	0.506	0.027	0.266	0.028	0.236	0.075	0.412	<u>0.022</u>	0.158	0.027	0.499	<b>0.012</b>
	MAE@40%	0.028	0.030	0.030	0.051	0.031	0.066	0.281	0.038	0.232	0.031	0.153	0.029	0.120	0.058	0.194	<u>0.024</u>	0.089	0.042	0.188	<b>0.023</b>
	MSE@40%	0.116	0.054	0.066	0.266	0.070	0.722	1.072	0.083	0.267	<u>0.035</u>	0.937	0.045	0.526	0.185	1.835	0.038	0.093	0.064	1.200	<b>0.028</b>
	MAE@60%	0.038	0.044	0.041	0.053	0.223	0.089	0.210	0.056	0.159	0.041	0.118	0.040	0.089	0.086	0.228	<u>0.032</u>	0.060	0.048	0.133	<b>0.030</b>
	MSE@60%	0.109	0.054	<u>0.059</u>	0.258	0.667	1.185	1.412	0.197	0.184	0.065	0.700	0.110	0.496	0.465	2.348	0.062	0.073	0.139	1.248	<b>0.047</b>
	MAE@70%	0.049	0.048	0.045	0.058	0.271	0.107	0.174	0.075	0.135	0.046	0.079	0.052	0.067	0.111	0.249	<u>0.041</u>	0.055	0.056	0.090	<b>0.038</b>
	MSE@70%	0.104	<u>0.102</u>	0.105	0.296	0.669	1.655	1.684	0.374	0.187	0.091	0.287	0.184	0.258	0.888	2.405	0.135	0.075	0.230	0.510	<b>0.091</b>

## Revisiting Multivariate Time Series Forecasting with Missing Values

Table 16. Performance comparison on six additional datasets with varying missing rates. The best results are highlighted in **Bold**.

Data	Metric	SegRNN	WPMixer	iTransformer	PatchTST	DLinear	PAttn	CSDI	NeuralCDE	ImputeFormer	TimesNet	Ours
ETTh2	MAE@0%	0.096	0.095	0.098	0.096	0.098	0.096	0.113	0.197	0.101	0.097	<b>0.094</b>
	MSE@0%	0.024	0.024	0.025	0.024	0.025	0.025	0.033	0.074	0.026	0.025	<b>0.023</b>
	MAE@20%	0.115	0.116	0.115	0.109	0.142	0.116	0.255	0.244	0.122	0.121	<b>0.107</b>
	MSE@20%	0.031	0.030	0.033	0.030	0.040	0.033	0.192	0.105	0.034	0.033	<b>0.028</b>
	MAE@40%	0.148	0.147	0.298	0.215	0.181	0.289	0.404	0.276	0.140	0.153	<b>0.131</b>
	MSE@40%	0.047	0.045	0.180	0.125	0.065	0.173	0.399	0.134	0.049	0.048	<b>0.039</b>
	MAE@60%	0.183	0.202	0.270	0.216	0.253	0.243	0.618	0.347	0.173	0.209	<b>0.154</b>
	MSE@60%	0.072	0.086	0.170	0.121	0.135	0.133	0.840	0.210	0.061	0.092	<b>0.055</b>
	MAE@70%	0.205	0.218	0.218	0.186	0.325	0.196	0.798	0.413	0.174	0.246	<b>0.172</b>
	MSE@70%	0.093	0.104	0.111	0.083	0.228	0.085	1.303	0.303	0.071	0.132	<b>0.069</b>
ETTm1	MAE@0%	0.2265	0.2405	0.2309	0.2379	0.2772	0.2423	0.4759	0.3331	0.2999	0.2100	<b>0.2000</b>
	MSE@0%	0.2302	0.2741	0.2514	0.2648	0.3504	0.2782	0.8854	0.4218	0.2682	0.2018	<b>0.2008</b>
	MAE@20%	0.2616	0.2900	0.2909	0.2779	0.3711	0.2971	0.5198	0.3809	0.3271	0.2584	<b>0.2368</b>
	MSE@20%	0.3068	0.3593	0.3751	0.3486	0.5499	0.3864	0.9345	0.5177	0.3282	0.2992	<b>0.2586</b>
	MAE@40%	0.3005	0.3308	0.3593	0.3456	0.4418	0.3592	0.5787	0.4391	0.3571	0.3040	<b>0.2734</b>
	MSE@40%	0.4007	0.4645	0.4851	0.4671	0.7412	0.4801	1.0499	0.6643	0.4749	0.4093	<b>0.3382</b>
	MAE@60%	0.3678	0.4171	0.4365	0.4091	0.5551	0.4191	0.7038	0.5457	0.4315	0.3993	<b>0.3414</b>
	MSE@60%	0.5960	0.7328	0.7580	0.6769	1.1067	0.7022	1.3801	0.9573	0.6978	0.6525	<b>0.5200</b>
	MAE@70%	0.4266	0.4863	0.5034	0.4743	0.6508	0.4816	0.8287	0.6278	0.4845	0.4828	<b>0.4013</b>
	MSE@70%	0.8006	0.9928	1.0663	0.9325	1.4721	0.9837	1.7733	1.2710	0.9035	0.8988	<b>0.6956</b>
ETTm2	MAE@0%	0.0802	0.0821	0.0781	0.0824	0.0918	0.0828	0.1313	0.1327	0.0813	0.0782	<b>0.0746</b>
	MSE@0%	0.0175	0.0182	0.0161	0.0182	0.0217	0.0187	0.0410	0.0363	0.0160	0.0165	<b>0.0152</b>
	MAE@20%	0.0956	0.1059	0.1020	0.1005	0.1405	0.1024	0.2687	0.1760	0.0888	0.1087	<b>0.0885</b>
	MSE@20%	0.0231	0.0266	0.0284	0.0251	0.0391	0.0278	0.1976	0.0591	0.0222	0.0260	<b>0.0203</b>
	MAE@40%	0.1159	0.1355	0.2673	0.2041	0.1743	0.2441	0.4131	0.1984	0.1088	0.1417	<b>0.1037</b>
	MSE@40%	0.0305	0.0394	0.1688	0.1210	0.0601	0.1490	0.4003	0.0765	0.0267	0.0406	<b>0.0258</b>
	MAE@60%	0.1432	0.1790	0.2651	0.2425	0.2412	0.2398	0.6221	0.2479	0.1360	0.1986	<b>0.1266</b>
	MSE@60%	0.0477	0.0685	0.1671	0.1423	0.1215	0.1448	0.8293	0.1194	0.0424	0.0811	<b>0.0384</b>
	MAE@70%	0.1650	0.1899	0.1905	0.1803	0.3104	0.1728	0.8024	0.3130	0.1602	0.2317	<b>0.1467</b>
	MSE@70%	0.0619	0.0808	0.0861	0.0779	0.2056	0.0717	1.2968	0.1857	0.0569	0.1142	<b>0.0520</b>
Weather	MAE@0%	0.031	0.030	0.030	0.031	0.034	0.031	0.051	0.051	0.035	0.028	<b>0.028</b>
	MSE@0%	0.021	0.019	0.018	0.019	0.023	0.020	0.042	0.029	0.020	0.016	<b>0.016</b>
	MAE@20%	0.042	0.050	0.044	0.048	0.099	0.046	0.173	0.073	0.041	0.062	<b>0.038</b>
	MSE@20%	0.028	0.025	0.031	0.027	0.045	0.032	0.220	0.036	0.028	0.033	<b>0.025</b>
	MAE@40%	0.050	0.074	0.152	0.150	0.135	0.157	0.300	0.095	0.051	0.088	<b>0.050</b>
	MSE@40%	0.037	0.036	0.167	0.156	0.078	0.140	0.500	0.060	0.033	0.047	<b>0.033</b>
	MAE@60%	0.066	0.102	0.175	0.169	0.197	0.168	0.466	0.150	0.066	0.128	<b>0.062</b>
	MSE@60%	0.061	0.062	0.223	0.169	0.178	0.163	1.099	0.150	0.064	0.089	<b>0.057</b>
	MAE@70%	0.076	0.121	0.101	0.118	0.254	0.100	0.586	0.204	0.076	0.166	<b>0.070</b>
	MSE@70%	0.081	0.084	0.138	0.128	0.318	0.120	1.707	0.284	0.083	0.154	<b>0.075</b>
Exchange	MAE@0%	0.0185	0.0187	0.0190	0.0186	0.0205	0.0187	0.0264	0.3223	0.0344	0.0195	<b>0.0184</b>
	MSE@0%	0.0010	0.0010	0.0010	0.0010	0.0011	0.0010	0.0017	0.1724	0.0031	0.0011	<b>0.0009</b>
	MAE@20%	0.0292	0.0324	0.0288	0.0273	0.0795	0.0227	0.1992	0.2969	0.0364	0.0458	<b>0.0217</b>
	MSE@20%	0.0031	0.0024	0.0024	0.0019	0.0126	0.0016	0.2089	0.1592	0.0029	0.0041	<b>0.0016</b>
	MAE@40%	0.0629	0.0783	0.1899	0.1416	0.1469	0.1408	0.4358	0.3326	0.0431	0.0786	<b>0.0253</b>
	MSE@40%	0.0129	0.0127	0.0770	0.0884	0.0429	0.1047	0.5718	0.2146	0.0034	0.0130	<b>0.0015</b>
	MAE@60%	0.1165	0.1364	0.2439	0.1978	0.2599	0.1283	0.7911	0.4334	0.0608	0.1357	<b>0.0363</b>
	MSE@60%	0.0363	0.0405	0.1060	0.1129	0.1394	0.0831	1.3714	0.3814	0.0071	0.0404	<b>0.0031</b>
	MAE@70%	0.1418	0.1836	0.2865	0.1321	0.3778	0.0718	1.0766	0.5412	0.0846	0.1991	<b>0.0517</b>
	MSE@70%	0.0490	0.0697	0.1413	0.0581	0.3011	0.0169	2.2850	0.5912	0.0128	0.0881	<b>0.0058</b>
BeijingAir	MAE@0%	0.2552	0.2571	0.2606	0.2609	0.2707	0.2601	0.3431	0.3167	0.2533	0.2583	<b>0.2526</b>
	MSE@0%	0.3026	0.3085	0.3156	0.3008	0.3263	0.3102	0.5141	0.3779	0.3189	0.2939	<b>0.2929</b>
	MAE@20%	0.2849	0.2896	0.2923	0.2866	0.3204	0.2949	0.4035	0.3478	0.2770	0.2922	<b>0.2758</b>
	MSE@20%	0.3467	0.3651	0.3655	0.3421	0.3853	0.3603	0.6010	0.4196	0.3496	0.3488	<b>0.3317</b>
	MAE@40%	0.3188	0.3312	0.3545	0.3278	0.3620	0.3480	0.4714	0.3950	0.3297	0.3322	<b>0.3106</b>
	MSE@40%	0.4285	0.4601	0.4820	0.4305	0.4760	0.4689	0.7584	0.5474	0.4645	0.4422	<b>0.4120</b>
	MAE@60%	0.3860	0.4011	0.4124	0.3976	0.4362	0.4142	0.5930	0.4750	0.4006	0.4017	<b>0.3728</b>
	MSE@60%	0.5939	0.6503	0.6573	0.6458	0.6799	0.6624	1.1378	0.7803	0.6110	0.6275	<b>0.5862</b>
	MAE@70%	0.4412	0.4632	0.4691	0.4613	0.5022	0.4673	0.7057	0.5456	0.4549	0.4789	<b>0.4337</b>
	MSE@70%	<b>0.7595</b>	0.8730	0.8874	0.8540	0.9358	0.8745	1.5761	1.0151	0.8327	0.9234	0.8010